



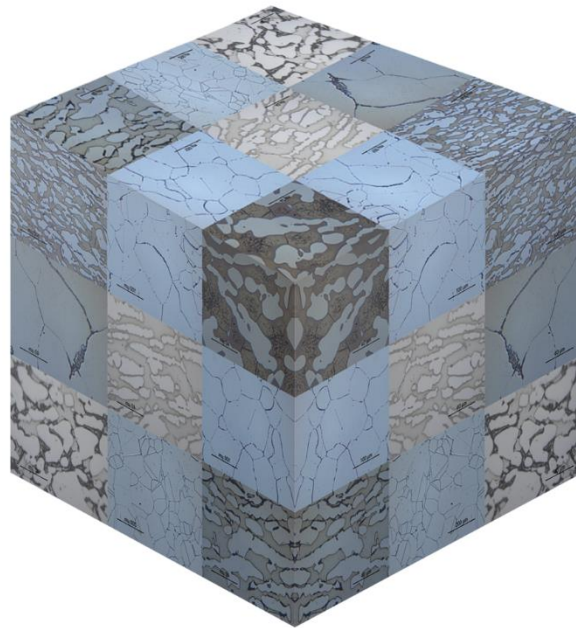
Universitetet
i Stavanger

DET TEKNISK-NATURVITENSKAPELIGE FAKULTET

MASTEROPPGAVE

Studieprogram/spesialisering: Masterprogram i konstruksjonsteknikk og materialteknologi. Spesialisering i offshorokontruksjoner	Vår semesteret, 2015 Åpen / Konfidensiell
Forfatter: Andreas Skaare (signatur forfatter)
Fagansvarlig: Torfinn Havn Veileder: Torfinn Havn	
Tittel på masteroppgaven: Rustfritt stål: Gjenvinning av akseptabel kvalitet etter eksponering overfor uønskede faser Engelsk tittel: Stainless steel: Recovery of properties after exposure to detrimental phases	
Studiepoeng: 30	
Emneord: Super duplex, 25Cr, UNS S32760 Super austenitic, 6Mo, 254SMO, UNS S31254 Stainless steel Secondary phases, sigma phase, quenching	Sidetall: 34 + vedlegg/annet: 18 Stavanger, 12/06-2015 dato/år

Stainless steel: Recovery of properties after exposure to detrimental phases



Andreas Skaare

Master Thesis

Faculty of Science and Technology

University of Stavanger

TITLE

TITLE

Stainless steel: Recovery of properties after exposure to detrimental phases

ABSTRACT

High alloyed stainless steel provides a desirable combination of corrosion resistance and mechanical properties, being a preferred material when ductility, overall strength and resistance to harsh environments are required.

High service temperatures where alloy elements, as chromium and molybdenum, are present, is a well-known recipe for the precipitation of detrimental phases in the material. Even a small amount of these precipitations may impair the mechanical and corrosion properties.

The main objective with this thesis is to investigate the possibility to recover the initial properties after detrimental phases have transformed part of the materials microstructure. Different stages of detrimental phases are intentionally provoked to achieve a wider spectra of analysis.

In order to quantify the damage and recovery, material is evaluated metallographically and by performing Charpy V-notch impact test, where the first mentioned gives us the exact amount of sub phases that has appeared in the microstructure and the latter gives us an idea of the behavior of the material, due to a sharp decrease in toughness led by the growth of detrimental phases in the given structure.

The theory behind steel restructuration proves to be right, showing that the microstructure and any detrimental phases can be dissolved by performing a correct heat treatment at a sufficiently high temperature with the correct cooling.

The first material, UNS S32760, is able to recover up to 86% percent of its toughness no matter what the previous exposure to detrimental phases was.

All previous detrimental phases retreat when proper heat treatment is applied. The lack of toughness recovery is due to the precipitation of a new detrimental phase, chrome nitride. This precipitation is due to the saturation of nitrogen in ferrite grains when a fast cooling is applied.

Samples from the second material, UNS S31254, were subjected to the same heat treatments. Results show lower propensity to formation of detrimental phases and an overall recovery of the microstructure compared to factory standards.

PREFACE

PREFACE

This report was written at the University of Stavanger (UiS) in the spring 2015. This work completes a two years Master of Science degree program in “Construction technique and Materials technology”, with specialization in offshore construction.

It is anticipated that the reader of this report has some technological background. All the features of high alloy stainless steel has not been presented, but only a brief introduction to each topic is given.

I wish to express my gratitude to Prof. Torfinn Havn for his inspiration, suggesting such an interesting topic and Ms. Ingunn Cecilie Oddsen for her useful guidance in the metallographic laboratory at the University of Stavanger.

I will also thank Lene Anita Marken and Erlend Andre Sandvik for always having time to answer my questions and for suggestions during the execution of this report.

I want to express my gratitude to Scandinavian Fittings and Flanges AS which supplied high alloy stainless steel to investigate and the University of Stavanger for providing all necessary equipment to be able to realize this research.

Stavanger, July 12, 2015

Andreas Skaare

FIGURES

FIGURES

Figure 1-Schaeffler diagram. X-axis is Cr-equivalent= $\%Cr+\%Mo+1,5*\%Si+0,5*\%Nb$. Y-axis is Ni-equivalent= $\%Ni+30*\%C+30*\%N+0,5*\%Mn$	3
Figure 2-Increasing nickel content changes the microstructure of stainless steel from ferritic to austenitic. (7).....	4
Figure 3-Isothermal time-temperature-transition for UNS s31803. Detrimental phases are presented as curves and show when the precipitation will take place.....	8
Figure 4-Different quenching mediums affects cooling rate and whether microstructure precipitates to secondary phases or not.	8
Figure 5-Standard full size Charpy V-notch specimen. Permissible variations are shown.	9
Figure 6- Transformation from pipe to test piece.....	10
Figure 7-Machined duplex steel ready for Charpy V-notch Impact test.....	10
Figure 8-Theoretical and experimental cooling in air medium.....	11
Figure 9-Theoretical and experimental cooling in water medium.....	12
Figure 10-All current heat treatments with the respective cooling ratio.....	14
Figure 11-Analysis procedure for metallographic evaluation and mechanical testing.....	16
Figure 12-500x magnification of microstructure of UNSs32760 before thermal treatment. Austenitic grain structure in lighter grey. Ferritic grain structure in darker grey. Distribution is 53% austenite / 47% ferrite.....	17
Figure 13-Sample 2 shows chrome nitride precipitations in thick ferrite grains. Precipitation is concentrated in the centre of the grain, away from austenite grains.....	18
Figure 14-Sample 1 shows sigma precipitations along grain boundaries after 12 minutes holding time.....	18
Figure 15-Sample 3 shows chrome nitride precipitations in the thick ferrite grains.....	19
Figure 16-Sample 4 shows a severe precipitation of sigma along boundaries and intergranularly after 23 minutes of holding time.....	19
Figure 17-Sample 5 shows chrome nitride precipitation intergranularly and between twin boundaries in all ferrite grains.....	20
Figure 18-Sample 6 shows a small amount of sigma precipitation after 1,2 minutes.....	20
Figure 19-Sample 7 shows a severe precipitation of chrome nitrides in the thicker ferrite grains.....	21
Figure 20-Sample 8 shows a concentration of sigma precipitation in the thinner ferrite grains.....	21
Figure 21-Relation between Charpy V-notch impact test results and the mileage of sigma phase.....	22
Figure 22-Relation between holding time in 1000 °C - 600 °C temperature range and mileage of sigma phase.....	23
Figure 23-Individual relation between toughness, percentage of damage and percentage of sigma phase.....	23
Figure 24-Sample 2. Two regions of the microstructure after 12 minutes holding time.....	25
Figure 25-Sample 1 after HT1 and HT5. No sign of secondary phases.....	25
Figure 26-Sample 3 after HT2 and HT5. No sign of secondary phases.....	26
Figure 27-Sample 4. Highlighted region with a consistent precipitation of secondary phases.....	26
Figure 28-Sample 8 after HT4.....	27
Figure 29-Sample 7 after HT4 and HT5.....	27

TABLES

Figure 30--Precipitation in relation with holding time. 1)Holding time 1,2min 2)Holding time 6min 3)Holding time 12min 4)Holding time 23min. 28

TABLES

Table 1-Detrimental phases. BCT (body centered tetragonal), BCC (body centered cube), cubic (primitive cubic)	6
Table 2-Chemical composition of UNS S32760 ref. Appendix D.....	7
Table 3-Chemical composition of UNS S31254 ref. Appendix E	7
Table 4-Overview of heat treatments performed on each sample. Thorough information is available in the beginning of chapter 3.2	14
Table 5-Toughness KV results in terms on Joules based on the average of three samples	17
Table 6-Loss of toughness in terms of percentage. Odd sample numbers are subjected to HT5, being rapidly cooled.	17

TABLE OF CONTENTS

TABLE OF CONTENTS

Title	I
Abstract	I
Preface	II
Figures	III
Tables	IV
Table of contents	V
1. Introduction.....	1
1.1. Part of the world to be studied.....	1
1.2. History of stainless steel	1
2. Theory	3
2.1. Stainless steel properties and its intermetallic phases	3
Molybdenum (Mo).....	4
Chromium (Cr).....	4
Nickel (Ni)	4
Nitrogen (N).....	5
Copper (Cu)	5
Sigma (σ) phase	5
Chi (χ) phase	6
Chrome nitride (Cr_2N)	6
2.2. UNSs32760.....	6
2.3. UNSs31254.....	7
2.4. Heat treatment.....	7
2.5. Charpy V-Notch impact test	9
2.6. Metallographic evaluation	9
3. Method	10
3.1. Machining.....	10
3.2. Heat treatment.....	11
3.3. Temperature variations	15
3.4. Charpy impact test	15
3.5. Metallographic evaluation	15
4. Results.....	16
4.1. UNS s32760 - Super duplex Stainless Steel.....	17

TABLE OF CONTENTS

Charpy V-notch impact test	17
Metallographic evaluation.....	17
Holding time 12 minutes – Temperature range 1000 °C - 600 °C.....	18
Holding time 23 minutes – Temperature range 1000 °C - 600 °C.....	19
Holding time 1,2 minutes – Temperature range 1000 °C - 600 °C.....	20
Holding time 6 minutes – Temperature range 1000 °C - 600 °C.....	21
Observations	22
4.2. UNS S31254 – Super austenite stainless steel.....	25
Metallographic Evaluation.....	25
Holding time 12 minutes – Temperature range 1000°C - 600°C.....	25
Holding time 23 minutes – Temperature range 1000°C - 600°C.....	26
Holding time 6 minutes – Temperature range 1000°C - 600°C.....	27
Observations	28
4.3. Uncertainties and errors	29
5. Discussion	30
6. Conclusion	32
References	33
Appendix	1
Appendix A. Charpy V-notch Impact test clarification and results.....	2
Appendix B. Calculations regarding theoretical approach for cooling ratio and experimental data for cooling processes	4
Appendix C. MDS 630 – NORSOK’s Material data sheet for UNS s32760 and UNS s31254.....	6
Appendix D. Inspection certificate UNS S32760	9
Appendix E. Inspection certificate UNS S31254.....	11
Appendix F. Schematic representation of sigma phase precipitation.....	13
Appendix G. Equipment	15
Appendix H. Organization of samples for further studies	18

INTRODUCTION

1. INTRODUCTION

1.1. PART OF THE WORLD TO BE STUDIED

The last decade tendency of the crude oil, reaching its price climax in 2011, has been the main reason for the oil exploration to move to remote locations where harsh environments are present. The industry is digging deeper for unknown reserves, making them recoverable due to new technologies.

Deepwater production facilities sets new requirements to the material selection. The expectation of performing under high pressures and to withstand higher temperatures than before, makes commonly used materials in the oil industry inappropriate for certain tasks.

Harsh environments, where low temperatures, sea currents and rugged seabed are present, make pipelines and risers vulnerable to vortex shedding and wave impacts, increasing the demand of fatigue- and high pressure- resistance. From a material perspective, we also have to deal with the concentration of corrosive agents in the surroundings of the well.

If above all these situations we remark the high cost of component failure and the tendency of extending the life span of the production facilities to make them economically interesting, we end up with a small selection of materials to meet all these requirements. It's now the stainless steels can show their brilliance (1).

1.2. HISTORY OF STAINLESS STEEL

Stainless steel was invented early in the 20th century when it was discovered that a certain amount of chromium made the material highly weather resistant. Being an alloy, where several elements are combined, opened for further investigation. Several attempts were considered and nowadays it is systematically organized according to chemical composition and given microstructure.

There are five stainless steel families: ferritic, martensitic, precipitation hardening, duplex and austenitic. In this report we will focus on the last two.

The early pioneers of stainless steel were people related to both science and industry. Focus was set on elements relation of iron-chromium and iron-chromium-nickel alloys, instead of the purpose of achieving a given structure. The difference of the stainless steel families were a collateral discovery from the relation between alloy content in the composition.

A later introduction of more sophisticated and accurate equipment set new standards to the alloys.

The introduction of the Vacuum oxygen decarburization (VOD) and Argon oxygen decarburization (AOD) in the 1970's, a process where the alloy is subjected to decarburization, reduction and desulphuration, developed sustainably the refining process leading to a significant improvement in the properties of alloy steels. (2)

Extensive studies were carried out the next two decades, focusing on the manufacturing and kinetics. Hot workability, weldability and corrosion resistance were main areas of interest in the thermal treatment.

INTRODUCTION

For austenitic stainless steel, it is truly believed that the detailed study of iron-chromium-nickel alloys made by Léon Guillet in the early 20th century set the standard. Differences in the chemical composition compared to what is implemented nowadays lie in the adopted refinements decades later.

(3)

The origin of austenitic-ferritic stainless steel (known as duplex steel) goes back to 1933, when a French foundry company produced by error a 20%Cr – 8%Ni – 2,5% Mo steel containing a high fraction volume of ferrite in an austenitic matrix. Unique corrosion resistance made this accidental alloy steel popular and is seen as the start of what we today know as the Duplex steel.

Notwithstanding the French origin, similar compositions were studied, patented and marketed simultaneously in Sweden and the United States.

In 1950 the UR 50 grade was presented by “Compagnie des Ateliers et Forges de la Loire”, a two-phase austenitic-ferritic steel with high yield strength and excellent corrosion resistance. Its properties made this steel a good contender for applications in the chemical industry, salt production, oil refining, pharmaceutical, etc. The same company presented also a proposed Duplex grade with a 0,2% N content.

In this decade, the production were done by high frequency induction furnaces, which basically melted the alloying elements without any refining. Lack of precision during production and rudimentary equipment made it difficult to achieve low oxygen, sulphur and carbon levels, making the duplex steels brittle during service.

Extensive studies were carried out the next two decades, focusing on the “hot workability, weldability and corrosion resistance and on their response to thermomechanical treatments”.

From the 80s, a new generation of duplex grades appeared, where nitrogen had a central role improving the weldability. From this moment, duplex steel suddenly became more widely used, offering better corrosion resistance and strength-to-weight ratio than 316 and 317 steels. Still, the extra cost did not always justify the benefits of choosing duplex, so the steel grade went in two different ways. Lean duplex appeared to avoid the overspecification, defined by low-nickel and low-molybdenum reducing alloy costs. Meanwhile, the other development of the grade was superDuplex and hyperDuplex, “driven primarily by the need for material that can partially replace more expensive alloys in the severest applications in the offshore oil and gas, chemical and petrochemical industries”. (4)

2. THEORY

2.1. STAINLESS STEEL PROPERTIES AND ITS INTERMETALLIC PHASES

Stainless steels are a versatile term to describe a family of engineering materials known primarily for their corrosion resistance properties.

A theoretical way of comparing them is with the Pitting Resistance Equivalent Number (PREN). It is a measure based on the chemical composition of the alloy, where the elements chromium, molybdenum and nitrogen determine a respective PREN-value. A high PREN-value indicates better corrosion resistance. Alloys with values above 32 are considered seawater-resistant, and a minimum of 40 is set for offshore purposes.

$$PREN = \%Cr + 3,3 \cdot \%Mo + 16 \cdot \%N$$

Equation 1-PREN-values above 40 are a minimum for offshore purposes [NORSOK M-630].

Weight percentage of chromium, molybdenum and nitrogen are deciding elements for the theoretical pitting resistance.

Common properties is that all materials embraced by this term have a minimum of 10,5% chromium and they principally contain iron.

(5)

Constitution of the desired microstructure at ambient temperature can be predicted using Schaeffler diagram, following rapid cooling from solution anneal temperature. Phase fields are shown in terms of nickel and chromium equivalents, and are based on the chemical composition. (6)

Duplex stainless steel is characterized by a two phase structure consisting of an equal mixture of austenite and ferrite grains. A desirable combination of mechanical properties and corrosion resistance is obtained by a thorough control of the chemical composition and the quenching¹ ratio from the annealing temperature to ambient temperature.

Austenitic stainless steel is characterized by a single phase structure consisting only of austenite grains, providing good corrosion resistance and simultaneously being non-magnetic, due to the lack of ferrite grains in microstructure.

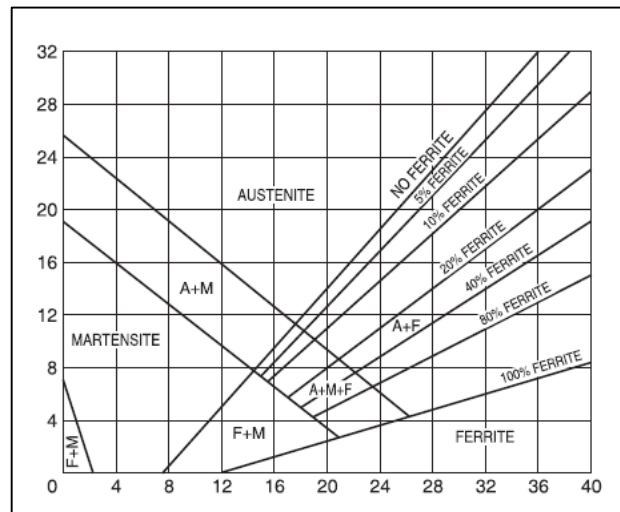


Figure 1-Schaeffler diagram. X-axis is Cr-equivalent= $\%Cr + \%Mo + 1,5 \cdot \%Si + 0,5 \cdot \%Nb$. Y-axis is Ni-equivalent= $\%Ni + 30 \cdot \%C + 30 \cdot \%N + 0,5 \cdot \%Mn$

¹ Rapid cooling of a work piece to obtain certain material properties.

THEORY

A major concern with the steel and its chemical composition is the formation of unwanted intermetallic phases. A correct cooling plays an important role, but so does the alloying elements:

MOLYBDENUM (MO)

Mo enhances the pitting corrosion resistance, being really effective with Cr contents above 18%. Mo is a ferrite former and increases the tendency of formation of detrimental intermetallic phases².

CHROMIUM (CR)

The corrosion resistance increases in relation with the amount of Cr. A minimum of 10% is necessary to form a stable passive film that can protect against atmospheric corrosion.

Cr increases the oxidation resistance at elevated temperatures, influencing the formation of oxide layer resulting from heat treatment.

Cr is a ferrite former, promoting a body centered cubic structure of the iron, and therefore Nickel is necessary to form the desired austenitic-ferritic-structure.

NICKEL (Ni)

Being an austenite stabilizer, it promotes the formation of a face-centered cubic structure. By increasing its weight% in the composition, ferritic structure changes over to austenitic.

Ni gives excellent toughness properties and delays the formation of intermetallic phases in duplex steels.

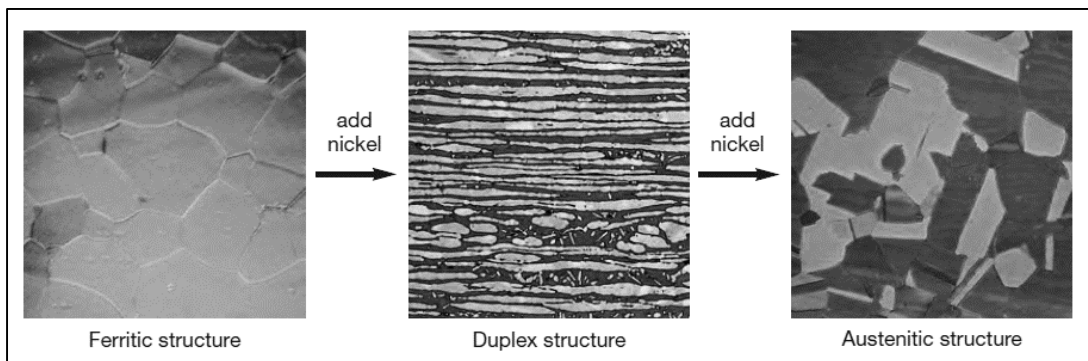


Figure 2-Increasing nickel content changes the microstructure of stainless steel from ferritic to austenitic. (7)

² Precipitations in microstructure that has a deteriorating effect on material. Synonyms in the report are: Detrimental phases, intermetallic phases, secondary phases.

THEORY

NITROGEN (N)

N does not eliminate the formation of detrimental intermetallic phases, but delays it enough to permit processing and fabricate duplex steel.

Cr and Mn increases the solubility of nitrogen, which explains why super duplex grade contain more nitrogen than lower chromium variants. Said that, nitrogen partition is still affected by temperature. "During cooling, austenite formation occurs and the ferrite becomes rapidly saturated with nitrogen". The excess of nitrogen leads to enrichment in the austenite, having a positive reaction on the pitting and crevice corrosion resistance and making it similar in both phases.

COPPER (Cu)

Cu improves corrosion resistance in non-oxidizing environments, such as sulfuric acid. The usage is limited to around 2%, since higher levels tend to reduce ductility.

Recapitulating, Mo and Cr enriches the ferrite structure, while N, Ni and Cu enriches the austenite formation. (7)

During heat treatment, many structural changes can happen, mostly with the ferrite-phase, as it diffuses approximately 100 times faster than in austenite. The consequence is due to a less compact lattice in the body-centered cubic (BCC) structure of the ferrite. As already mentioned, the ferrite is enriched in Cr and Mo and shows great propensity for the formation of intermetallic phases. Furthermore, the solubility falls in relation with decreasing temperature, increasing the probability of precipitation formation in the structure.

For austenitic steels, face-centered cubic (FCC) lattice structure is always present above the critical temperature of 700°C and will normally break down to either ferrite, cementite or martensitic-structure. By increasing the alloy content, with such elements as manganese and nickel, the austenitic structure can be stable even at room temperature. Even by holding a stable microstructure during temperature changes, there is a propensity of forming chromium carbides along grain boundaries, reducing mainly the chromium content in the austenite grains.(8)

There are several secondary phases, but we will mainly look at the ones exposed in the 600 °C to 1000 °C temperature range. The presence of these precipitations are generally associated with a loss of mechanical properties and corrosion resistance. (9)

SIGMA (σ) PHASE

Sigma phase has its origin in the system of Fe and Cr, being a non-magnetic intermetallic compound with a complex tetragonal crystal structure. Alloys with Cr and Mo are unstable to this phase at temperatures between 600°C and 1000 °C.

The formation comes as a consequence of high temperature exposure or incorrect heat treatment, influencing the mechanical properties and corrosion resistance.

The mechanical properties are affected by a several loss of toughness, due to bad deformability of the phases because of their low fraction of metallic binding (10).

THEORY

The decrease of corrosion resistance is featured by the depletion of Cr and Mo around the area σ has precipitated.

For duplex stainless steel, this phase affects the ferrite structure, decomposing it and nucleating as sigma-particles with a high rate formation and in potentially large fraction volume.

For super austenitic stainless steel, the precipitation initiates in the delta ferrite/ austenite (δ/γ) boundary. As aging temperature increases, σ sigma and γ_2 secondary austenite tend to precipitate in δ delta-ferrite. (11) (12)

For illustrations on how σ precipitates, see Appendix F.

CHI (γ) PHASE

Chi-phase precipitates in smaller amounts at the ferrite grain boundaries, in the same temperature range but prior to sigma-phase precipitation. As an eutectoid reaction, chi-phase leads to further sigma- and secondary austenite-formation. (13) (2)

CHROME NITRIDE (Cr_2N)

High temperatures, above 1000°C, increase solubility of nitrogen in the ferrite phase. During fast cooling, saturation of nitrogen occurs.

At lower temperatures, N has low solubility in the ferrite phase. Saturation leads to precipitation of chrome nitrides, as a result of the short time interval N has to diffuse back to the austenite. (11) (2)

The presence of chromium nitrides in the microstructure have a detrimental effect on the material properties. They cause embrittlement of the material (see chapter 4.1 for results) and previous studies attribute a loss of corrosion resistance due to the depletion of Cr and N in the ferrite grains. (15)

Table 1-Detrimental phases. BCT (body centered tetragonal), BCC (body centered cube), cubic (primitive cubic)

<i>Type of precipitate</i>	<i>Nominal composition</i>	<i>Lattice type</i>	<i>Temperature range [°C]</i>
σ (sigma)	Fe 35-55, Cr 25-40, Mo 11-25	BCT	1000-600
X (chi)	Fe 35-55, Cr 25-40, Mo 11-25	BCC	1000-700
Chromium nitride	Cr_2N	Cubic	900-700

2.2. UNSS32760

Known as 25Cr Duplex, a super duplex stainless steel with excellent corrosion resistance and strength. It is produced and manufactured by Tubacex Tubos Inoxidables for Scandinavian

THEORY

Fittings and Flanges AS. This product is a seamless stainless steel tube, hot finished³, passivated and plain beveled ends. The raw material is processed in an electric furnace, AOD'ed and rapidly cooled. The result is a balanced microstructure with 53,70% ferrite content and the remaining of austenite.

The steel grade is made to meet the minimum PREn requirements for duplex steel, having a composition with good resistance against chlorides, organic and sulfuric acids.

Chemical composition:

Table 2-Chemical composition of UNS S32760 ref. Appendix D

%	C	Mn	Si	P	S	W	Ni	Cr	Mo	N	Cu	PREn
Avg.	0,018	0,68	0,51	0,024	0,0004	0,56	6,95	25,5	3,66	0,24	0,68	41,42

2.3. UNSS31254

This material is a super austenitic steel with high levels of nitrogen and molybdenum, known as 6Mo or 254SMO.

This alloy was the first austenitic stainless steel using nitrogen for added corrosion resistance. High nitrogen content gave it a superior resistance to chloride pitting and crevice corrosion, compared to earlier austenitic alloys. It is produced and manufactured by DMV Stainless France for Scandinavian Fittings and Flanges. The product is a seamless stainless steel tube, hot finished and annealed. (12) Raw material is melted in an electric furnace and decarburized with AOD or VOD.

Chemical composition:

Table 3-Chemical composition of UNS S31254 ref. Appendix E

%	C	Mn	P	S	Si	Ni	Cr	Mo	N	Cu	PREn
Min.						17,5	19,5	6,0	0,18	0,5	42,18
Max.	0,02	1,0	0,03	0,01	0,80	18,5	20,5	6,5	0,22	1,0	45,47
Avg.	0,02	1,0	0,03	0,01	0,80	18,0	20,0	6,25	0,2	0,75	43,83

2.4. HEAT TREATMENT

Correct thermal treatment is required to be able to achieve the desired corrosion and mechanical properties. Chromium and molybdenum are the principal elements to improve corrosion resistance, but also the main actors in the formation of detrimental phases in high alloy stainless steel. Increasing alloy content tends to move phase-curves to shorter times, accelerating precipitation reactions.

³ Process of deforming material through rollers at a temperature above its recrystallization temperature

THEORY

In order to obtain the desired microstructure, reaction kinetics must be taken to account.

Kinetics of detrimental phase precipitation in duplex steel are influenced by the chemical composition and the particular holding time in several temperature ranges. σ sigma phase has three distinct precipitation mechanisms:

- “Nucleation and growth from original ferrite”
- “Eutectoid⁴ decomposition of ferrite, forming σ and γ_2 secondary austenite”
- “ σ growth from austenite after total consumption of original ferrite” (15)

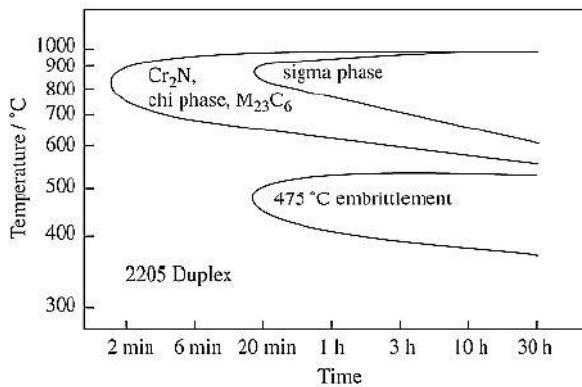


Figure 3-Isothermal time-temperature-transition for UNS s31803. Detrimental phases are presented as curves and show when the precipitation will take place.

254SMO belongs to the high performance austenitic stainless steel.

With a high content of chromium and molybdenum, chi and sigma precipitation is accelerated. Moreover, all precipitations occur in the austenite grain boundaries, in low volume, with a similar effect on the properties: loss of corrosion resistance. (11)

High alloy content makes both materials prone for formation of detrimental phases. Kinetics can be “controlled” by a proper quenching, by defining the cooling rate. A fast cooling rate is easily achieved by quenching in water medium, while air medium will decelerate the rate and reach the undesired noses from the detrimental precipitations.

Sigma and chi precipitations occurs at high temperatures at the same time as the chromium nitride precipitation. Sigma phase precedes chi formation, but precipitates in a greater volume. Both phases have similar effects on properties and are similar from a metallographic perspective.

For austenitic stainless steel, detrimental phase transformation is characterized by a slow transformation of chi and sigma.

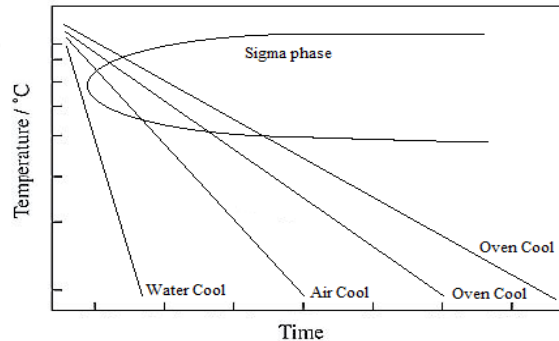


Figure 4-Different quenching mediums affects cooling rate and whether microstructure precipitates to secondary phases or not.

⁴ Reaction where a solid transforms into two other solid phases

THEORY

2.5. CHARPY V-NOTCH IMPACT TEST

The Charpy V-notch impact test is a standardized test which determines the amount of energy absorbed by the test material during fracture. This test works as a tool to quantify the temperature-dependent ductility⁵ of a given material, using the absorbed energy as a measure to determine its toughness.

From ASTM A370:

-19.1. “A Charpy V-notch impact test is a dynamic test in which a notched specimen is struck and broken by a single blow in a specially designed testing machine. The measured test values may be the energy absorbed, percentage of shear fracture”.

-21.1.1. “A Charpy impact machine is one in which a notched specimen is broken by a single blow or a freely swinging pendulum. The pendulum is released from a fixed height. Since the height to which the pendulum is raised prior to its swing, and the mass of the pendulum are known, the energy of the blow is predetermined”.

-22.1.2.2. “When the specification calls for a minimum average test result, three specimens shall be tested”.

-22.3. “The machining of the notch is critical, as it has been demonstrated that extremely minor variations in notch radius and profile, or tool marks at the bottom of the notch may result in erratic test data”

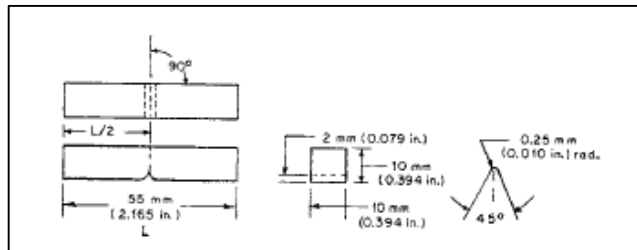


Figure 5-Standard full size Charpy V-notch specimen. Permissible variations are shown.

2.6. METALLOGRAPHIC EVALUATION

In this research, metallography is the study of the microscopic structure of the alloys using LOM (Light optical microscope). This analysis reveals how thermal treatment and alloy kinetics have transformed the microstructure and which phases have precipitated.

Depending on the desired outcome, several etchant methods are available. Depending on the alloy, a small selection of chemicals will be appropriate

Standard practice for microetching⁶ metals and alloys is presented in ASTM E407-99. It covers chemical solutions and procedures for etching.

Prior etching, surface must be uniformly polished, free of any surface deformation. In this respect mechanical polishing, a 1 μm diamond polish is considered as a minimum. Further literature around guidance to metallographic preparation of stainless steel is to be found in ASTM E3 – 01(2007)e1. (14)

⁵ Ability to deform under tensile stress.

⁶ Development of microstructure for observation with a microscope with higher magnification than 50x

METHOD

3. METHOD

The major part of this thesis has been focusing on the laboratory research. SFF provided the necessary material to perform several heat treatments, in order to get the desired results. The material came in 6 and 8 inches pipes with a wall thickness of 14 and 24 mm consequently.

3.1. MACHINING

With a liquid cooled saw, based on a mixture of water and oil, the first pipe element was split in half. From there single pieces with a small inner- and outer-bending radius were produced.

All singles pieces were milled into the correct measures and shape. 32 pieces with a cross section of 12x12 millimeters, and 4 pieces with a cross section of 10x10 millimeters ready to be analyzed for toughness with the Charpy V-notch Impact test.

During milling, in order to not expose the steel to undesired heat, each feeding removed a maximum of 500 micrometers of material while being continuously exposed to coolant. Last step prior to impact testing, was to mill into place the v-notch required by ASTM A370. An automated machine was used for this purpose, assuring correct measures.

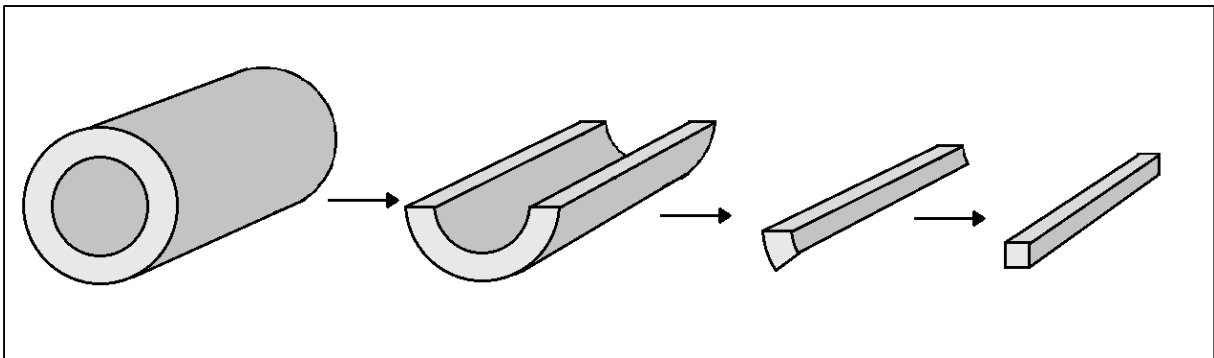


Figure 6- Transformation from pipe to test piece

General guidelines during machining of materials were:

- Use powerful and rigid machines
- Minimize vibration by keeping tool extension as short as possible
- Use adequate speed to avoid built-up edge and rapid wear
- Change tooling inserts at scheduled intervals
- Use generous flows of coolant at all time
- Apply uniform attaching pressure to avoid jamming

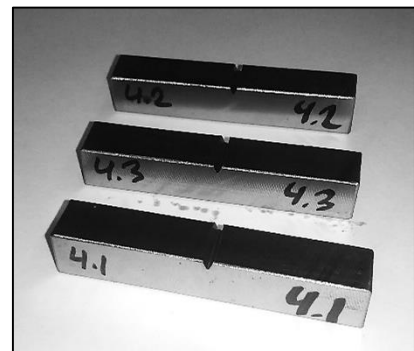


Figure 7-Machined duplex steel ready for Charpy V-notch Impact test

METHOD

3.2. HEAT TREATMENT

As mentioned in chapter 2.4, all heat treatments are based on the same principle of production of stainless steels. Different cooling rates, providing different holding times in the sigma-range temperatures, will not only provide a restructuring of the material, but also the growth of intermetallic phases.

To assure an accurate procedure during treatment, a data logger is connected to the test piece during all heat variation. The thermocouple in question is an EI-USB-TC-LCD logger with a K-element wired and welded to the test piece.

To assure accuracy of oven and thermocouple, thermodynamics theories were used to compare experimental data to the theoretical approach.

Two situations were considered:

- A test-piece, after reaching annealing temperature, cooled down in air.
- A test-piece, after reaching annealing temperature, cooled down in water.

First scenario is based on *Stefan-Boltzmann law* and shows an extraordinary similarity. The cooling is described as energy radiated per surface area of the body. As the temperature drops, conduction energy transfer for the area of the material that is in contact with the table comes in addition to the initial radiation transfer and might explain an accelerated cooling.

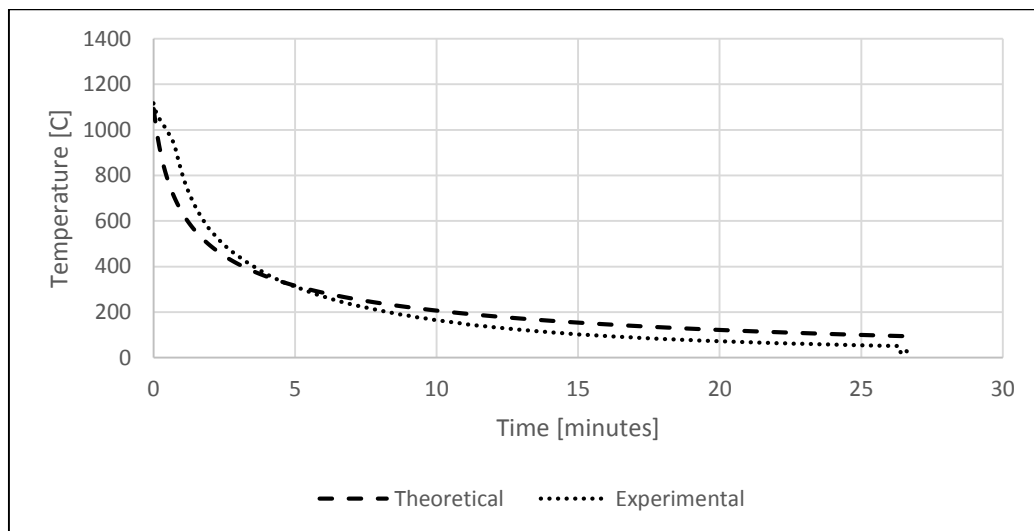


Figure 8-Theoretical and experimental cooling in air medium

As for the second scenario, Newton's Law of Cooling is used. It is basically a convective heat transfer, where the energy goes from one place to another by the movement of fluids.

The major issue here was to select the correct heat transfer coefficient for the water, as it goes from 500-10000 W/m²K. Several values were tried, where one in the midrange seemed to apply for the given situation.

METHOD

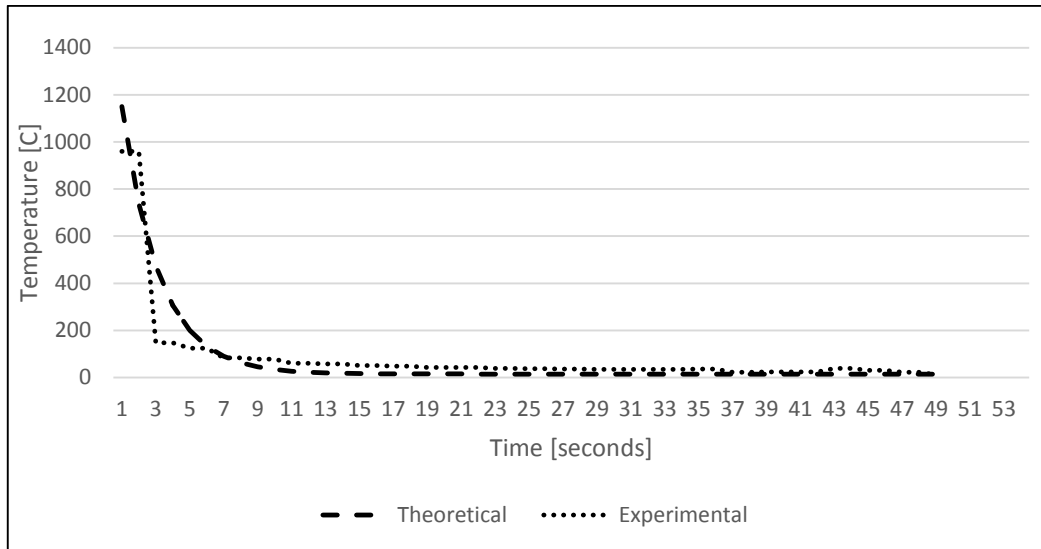


Figure 9-Theoretical and experimental cooling in water medium

Both situations show good similarity with theory. Combining these two thermodynamically laws can be useful in order to decide further controlled cooling.
See Appendix B for further information regarding calculations.

Earlier studies confirm that both materials are prone to detrimental phases the range of temperatures between 1000 °C and 600 °C. (15) (16) (2)

For all treatments, common aspects are:

- It took 8 minutes to reach solution anneal temperature after inserting materials
- All test pieces had a holding time of 30 minutes in solution anneal temperature

Equal heat treatments were performed on both materials, but with different solution anneal temperature.

Each material certificate stated the solution anneal temperature:

- UNSS32760, solution anneal temperature 1110 °C
- UNSS31254, solution anneal temperature 1150 °C/1250 °C

Five different exposures are achieved with different holding times and cooling methods.

1. First treatment, applied on all pieces marked as 1 and 2. (HT 1)
*8 minutes with high temperature until solution anneal temperature is reached.
Holding time in solution anneal temperature is 30 minutes.
Then, oven is turned off, and material is left inside until 50 °C is reached.*

Holding time 1000 °C-600 °C-region: 710 seconds (12minutes)

METHOD

2. Second treatment, applied on all pieces marked as 3 and 4. (HT 2)
*8 minutes with high temperature until solution anneal temperature is reached.
Holding time in solution anneal temperature is 30 minutes.
Then oven is set to reach 250 °C in 60 minutes.
After this, oven is turned off and material is taken out when 50 °C is reached.*

Holding time 1000 °C-600 °C-region: 1390 seconds (23 minutes)

3. Third treatment, applied on all pieces marked as 5 and 6. (HT 3)
*8 minutes with high temperature until solution anneal temperature is reached.
Holding time in solution anneal temperature is 30 minutes.
After this, material is taken out for air cooling.*

Holding time 1000 °C-600 °C-region: 70 seconds (1,2 minutes)

4. Fourth treatment, applied on all pieces marked as 7 and 8. (HT 4)
*8 minutes with high temperature until solution anneal temperature is reached.
Holding time in solution anneal temperature is 30 minutes.
Then, oven is turned off. Material stays inside oven for 510 seconds
(reaching 720 °C).
After this, material is taken out for air cooling.*

Holding time 1000 °C-600 °C-region: 375 seconds (6 minutes)

5. Fifth treatment, applied on pieces marked as 1, 3, 5 and 7. (HT 5)
*8 minutes with high temperature until solution anneal temperature is reached.
Holding time in solution anneal temperature is 30 minutes.
After this, material is rapidly cooled down in water.*

The purpose with this treatment is to eliminate all previous detrimental phases.

METHOD

Figure 10 shows the respective heat treatments the samples were subjected to in order to provoke undesired phases in the microstructure.

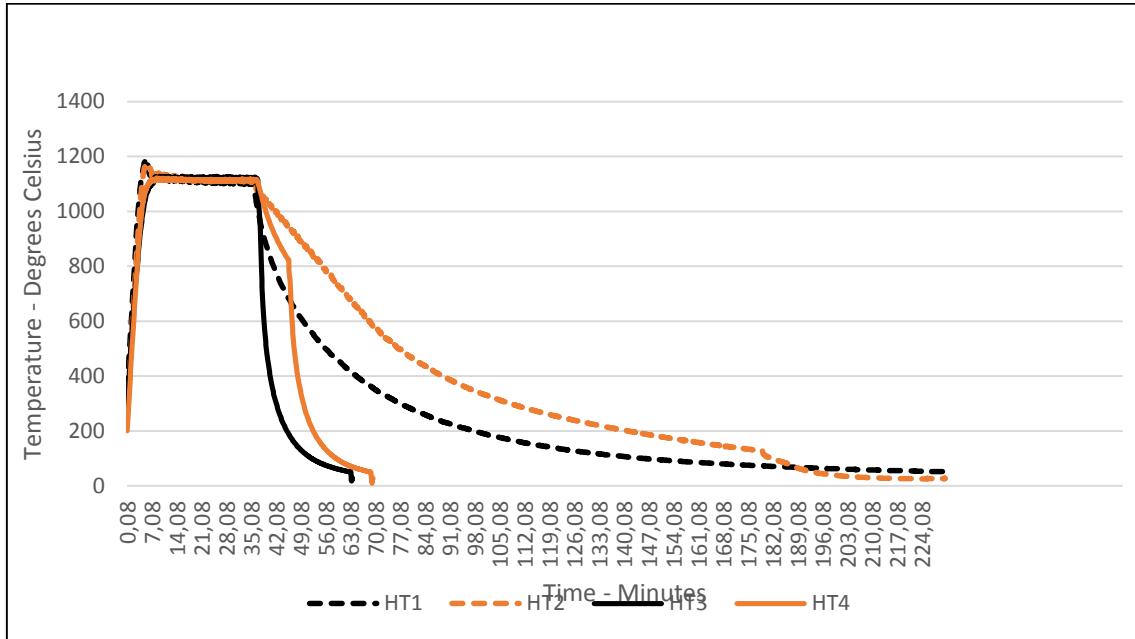


Figure 10-All current heat treatments with the respective cooling ratio

Through the presentation of the results, terminology as HT for heat treatment will be used. Table 4 shows a recapitulation of the variety of heat treatments performed. I.e. sample 1 has been subjected to heat treatment 1 and heat treatment 5.

Table 4-Overview of heat treatments performed on each sample. Thorough information is available in the beginning of chapter 3.2

Sample	Holding time in 1000°C to 600°C	HT 1 12 minutes	HT 2 23 minutes	HT 3 1,2 minutes	HT 4 6 minutes	HT 5 Rapidly cooled in water
1		X				X
2		X				
3			X			X
4			X			
5				X		X
6				X		
7					X	X
8					X	

METHOD

3.3. TEMPERATURE VARIATIONS

The theory behind cooling in air- and water-medium showed an extraordinarily resemblance with experimental data. All further adjustments during heat treatment were based on temperature measured from the thermocouple.

The oven was set to 1080 °C when the thermocouple marked between 1120 °C and 1140 °C.

Sample placement in the oven had a major significance for correct measurement. Samples were always placed in the middle of chamber, away from the heaters. This assured a uniform heating of the material.

3.4. CHARPY IMPACT TEST

A Zwick Roell RKP450 pendulum impact tester was used for Charpy impact test. Calibrated after ISO standards for 450 joules pendulum moment.

27 samples were collected and checked against dimension criterias specified in ASTM E370-08 [22.2.2], all being inside the permissible tolerances.

Test pieces were placed in ethanol in a freezer and cooled down to -46 °C prior testing.

See appendix A for all information regarding Charpy V-notch impact test.

3.5. METALLOGRAPHIC EVALUATION

Before etching, preparation was carried out by grinding (80, 120, 250, 400, 800, 1000 and 1400 grinding papers) and polishing with diamond pastes (3 and 1 µm).

For duplex steels, a combination of two etchant methods were chosen to achieve a good delineation of austenite/ferrite-, intermetallic- and chromium nitride-phases. Performed in sequence:

1. 10% Oxalic acid electrolytic⁷ – 5,5V for 20 seconds
2. 20% NaOH electrolytic – 2V for 6 seconds

For super austenitic steels, a 60% HNO₃ electrolytic – 2V for 20 seconds, gave the best result. I first tried a V2A @ 50 – 60 °C with 100 ml H₂O, 100 ml HCl and 10 ml HNO₃ for 120 seconds, but experienced bad grain delineation and a passive oxide layer.

Further analysis was carried out with a light optical microscope, saving pictures of each sample in 100x-, 200x- and 500x-magnification.

In order to quantify the content of detrimental phases, software “ImageJ” was used to facilitate the separation of phases in the microstructure. An illustration from the light optical microscope was analyzed manually by calculating the amount area of detrimental phase in respect to region of the illustration. The result is presented in terms of percentage.

⁷ Method of using a direct electric current to drive a chemical reaction

RESULTS

4. RESULTS

Results are presented with diagrams/charts gathered from the laboratory research. At the end of each chapter, concise observations related to the given information are stated.

“Test” refers to the part where the material has been evaluated without any form of heat treatment. The output information is used to set a bench mark in order to compare the state of further tested materials.

For all testing, material is ordered after the defined HT⁸.

Diagram 6 shows how it is proceeded for HT1, where test material 1 and 2 are selected.

The procedure is the same for the other HT, only changing the selected heat treatment and chosen samples (i.e. for HT2, test pieces 3 and 4 are selected).

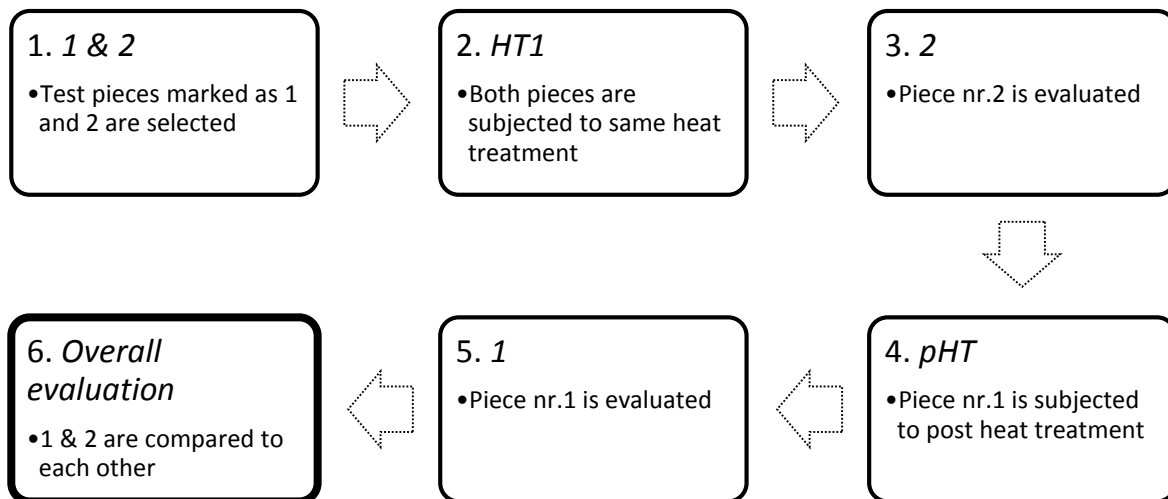


Figure 11-Analysis procedure for metallographic evaluation and mechanical testing

⁸ HT stands for heat treatment, and it is further used in this report.

RESULTS

4.1. UNS S32760 - SUPER DUPLEX STAINLESS STEEL

CHARPY V-NOTCH IMPACT TEST

Table 5-Toughness KV results in terms on Joules based on the average of three samples

Number test	1	2	3	4	5	6	7	8	
KV [J]	299,36	286,50	41,77	268,61	6,31	267,86	200,19	258,07	24,58

Table 5 shows the results from the Charpy test. All values are based on a average of three tests.

Table 6-Loss of toughness in terms of percentage. Odd sample numbers are subjected to HT5, being rapidly cooled.

Number test	1	2	3	4	5	6	7	8	
Damage [%]	0	4,3	86,04	10,27	97,89	10,52	33,13	13,79	91,79

Table 6 shows the variation of toughness. All percentages are based on the initial toughness measured on three samples of non heat treated alloy.

Odd sample numbers are subjected to the initial heat treatment and finally to heat treatment 5, rapidly cooled.

See Appendix A for further information

METALLOGRAPHIC EVALUATION

The pictures with odd numbers (1, 3, 5 and 7) are primarily free for sigma phase, but show a consistent precipitation of Cr₂N in ferrite grains. The pictures with even numbers (2, 4, 6 and 8) show different stages of sigma phase.

In the pictures:

- Ferrite grain is marked as α (alpha)
- Austenite grain is marked as γ (gamma)
- Sigma phase is marked as σ
- Chrome nitride is marked as β (beta)

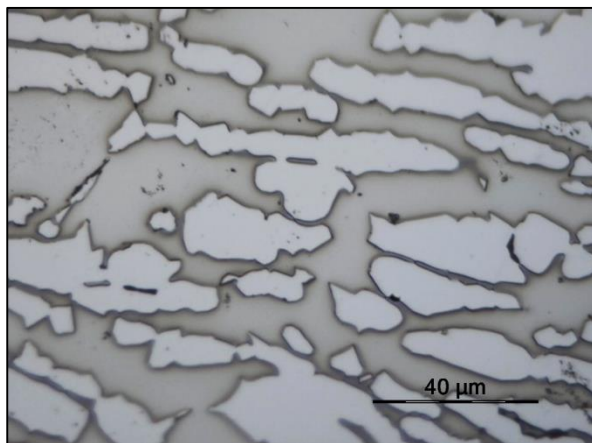


Figure 12-500x magnification of microstructure of UNSs32760 before thermal treatment. Austenitic grain structure in lighter grey. Ferritic grain structure in darker grey. Distribution is 53% austenite / 47% ferrite

RESULTS

HOLDING TIME 12 MINUTES – TEMPERATURE RANGE 1000 °C - 600 °C

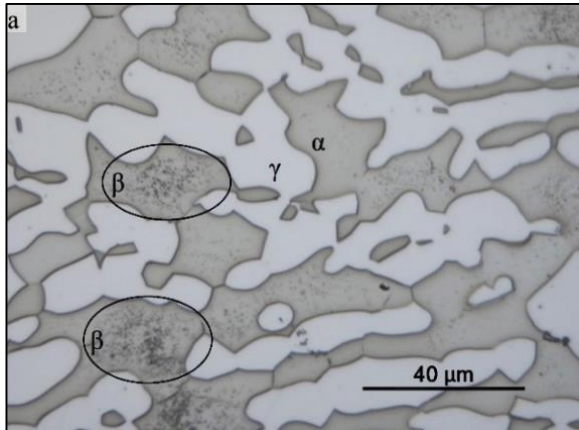


Figure 13-Sample 2 shows chrome nitride precipitations in thick ferrite grains. Precipitation is concentrated in the centre of the grain, away from austenite grains

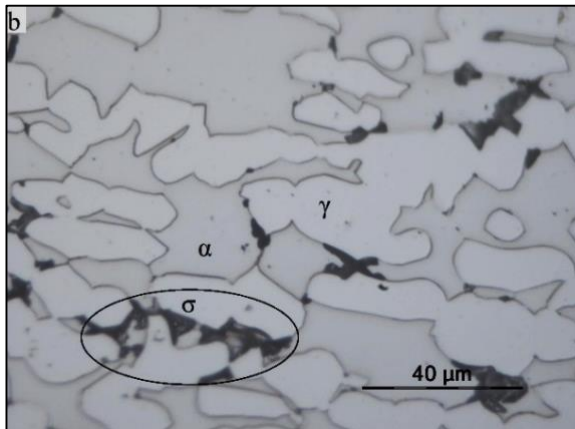


Figure 14-Sample 1 shows sigma precipitations along grain boundaries after 12 minutes holding time.

Figure 13 shows the result after a correct heat treatment (HT5).

All sigma precipitations are dissolved.

Marked as beta, shows precipitations of chrome nitrides concentrated in the middle of larger ferrite grains. During solution anneal, ferrite grains are saturated with nitrogen and larger grains does not manage to diffuse all nitrogen back to the austenite.

Figure 14 shows precipitation of sigma roughly calculated to be around 4,91% of the visible microstructure, after exposed to HT1.

In this picture, all black colored compounds are sigma precipitates. Smaller amounts of sigma are present in ferrite/austenite boundaries.

In the marked area, an initial precipitation in grain boundaries continued at incoherent twin boundaries and finally intergranularly.

RESULTS

HOLDING TIME 23 MINUTES – TEMPERATURE RANGE 1000 °C - 600 °C

Figure 15 shows precipitations of chrome nitrides in the thicker ferrite grains, mainly intergranularly. In the highlighted area a small amount of precipitation in the twin boundaries is visible as black lines in the marked area.

Figure 16 shows roughly 21,3% of sigma phase. In this situation the detrimental phase has grown intergranularly through the majority of the ferrite grains.

In the marked area there is a total depletion of ferrite grains.

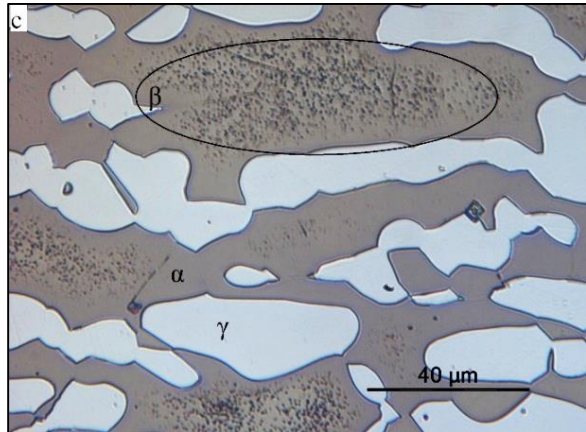


Figure 15-Sample 3 shows chrome nitride precipitations in the thick ferrite grains

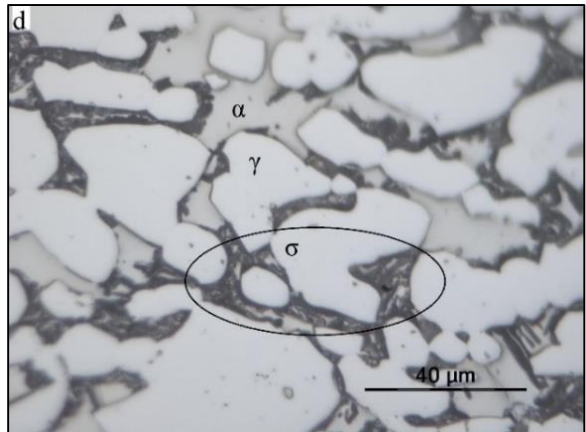


Figure 16-Sample 4 shows a severe precipitation of sigma along boundaries and intergranularly after 23 minutes of holding time

RESULTS

HOLDING TIME 1,2 MINUTES – TEMPERATURE RANGE 1000 °C - 600 °C

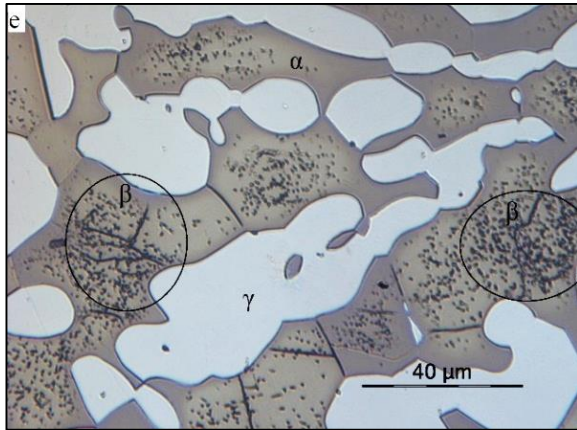


Figure 17-Sample 5 shows chrome nitride precipitation intergranularly and between twin boundaries in all ferrite grains

Figure 17 shows an evident precipitation of chrome nitride in twin boundaries of the ferrite and a consistent growth in the larger ferrite grains.

In figure 18 it is hard to differentiate between sigma- and chi- phase. This sample shows the lowest percentage of sigma precipitation, being 2,65%. Precipitation in small amounts between austenite/ferrite grains are possible chi-phase or early sigma. The upper part of the picture shows an amount of sigma phase precipitated intergranularly in ferrite/ferrite boundaries.

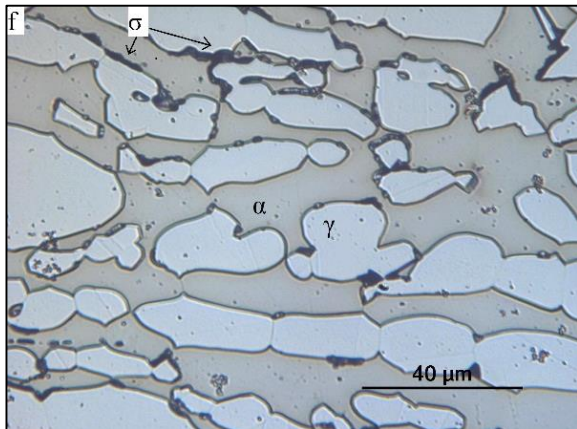


Figure 18-Sample 6 shows a small amount of sigma precipitation after 1,2 minutes

RESULTS

HOLDING TIME 6 MINUTES – TEMPERATURE RANGE 1000 °C - 600 °C

Figure 19 shows a severe precipitations of chrome nitrides. In the thicker ferrite grains the precipitation happened intergranularly with a higher concentration in the centre of the grain. In the thinner ferrite grains, precipitation in the twin boundaries is visible (black lines in the marked area).

Figure 20 is calculated to have around 5,1% sigma phase in its microstructure. It is concentrated in a specific area and precipitated intergranularly in thinner ferrite grains. Its concentration make the sample susceptible to loss of ductility, due to the lack of bonding energy between grains in that specific area.

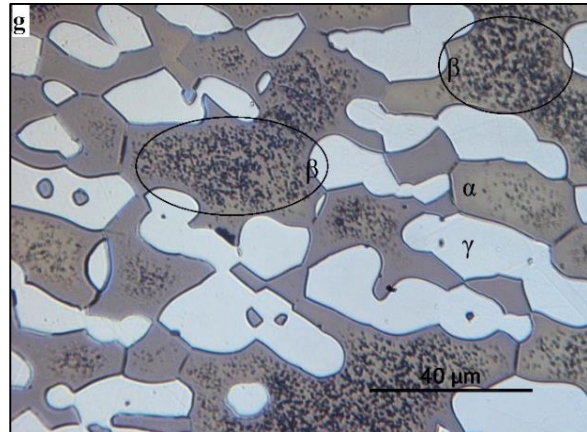


Figure 19-Sample 7 shows a severe precipitation of chrome nitrides in the thicker ferrite grains

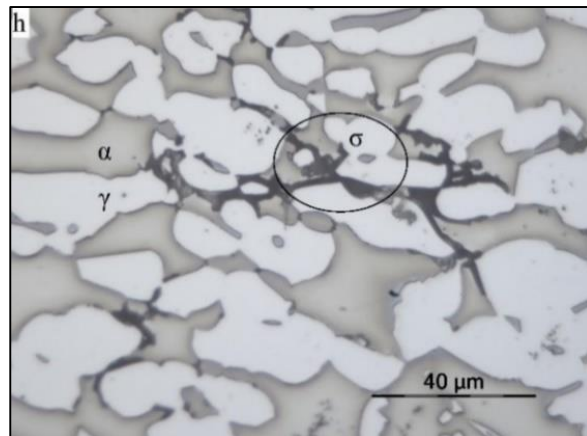


Figure 20-Sample 8 shows a concentration of sigma precipitation in the thinner ferrite grains

RESULTS

OBSERVATIONS

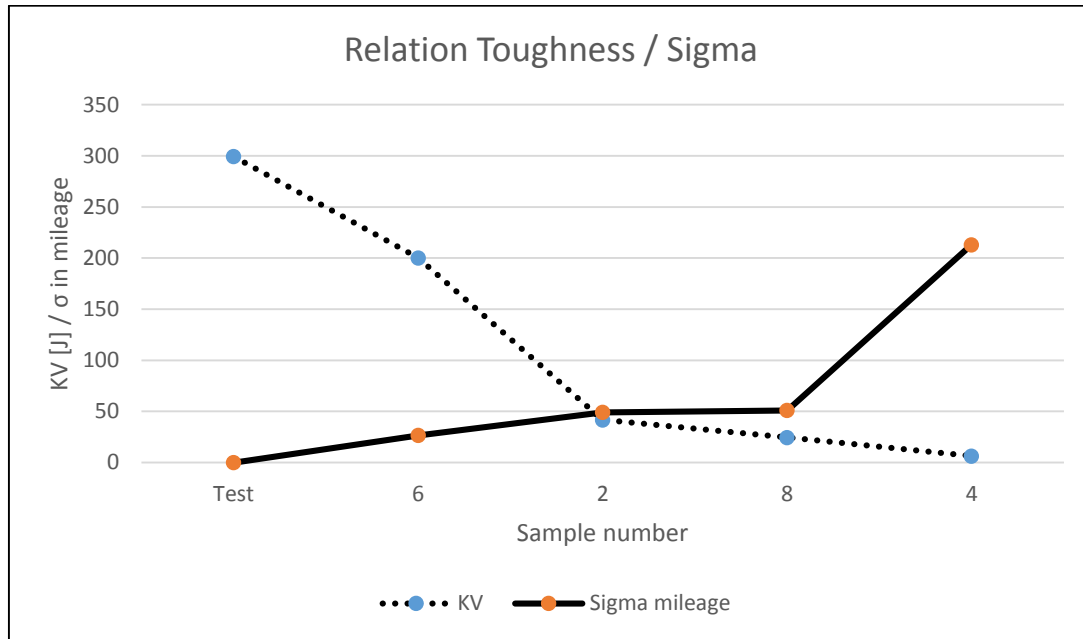


Figure 21-Relation between Charpy V-notch impact test results and the mileage⁹ of sigma phase

Figure 21 corroborates previous research behind the effect of σ precipitation. Tendency is clear, toughness decreases drastically as the precipitation of the detrimental phase increases. The remaining samples had no sign of σ precipitation. Precipitation of nitrogen in ferrite grains as Cr_2N shows a negative effect on toughness, reduced up to 13% compared to initial measurements.

⁹ Mileage is used in fig.24 and fig.25 to adjust the magnitude of the values to the diagrams. I.e. 50 mileage equals to 5%

RESULTS

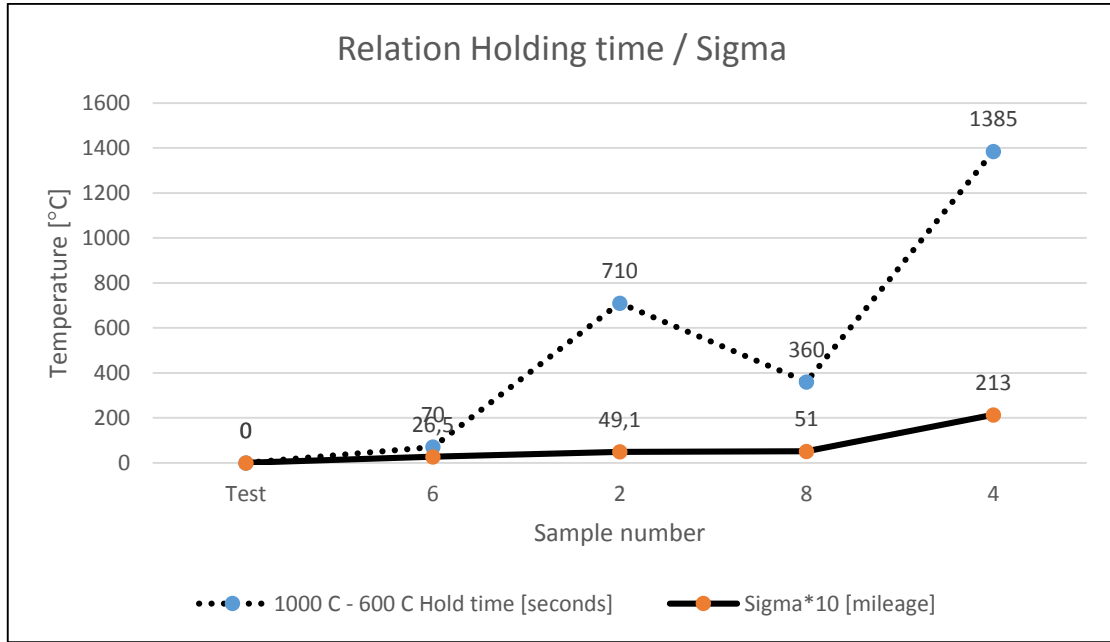


Figure 22-Relation between holding time in 1000 °C - 600 °C temperature range and mileage of sigma phase

Figure 22 shows the average effect an increasing holding time in the 1000 °C to 600 °C temperature range has on the precipitation rate of σ phase. Both variables increase exponentially with a different magnitude in respect to each other.

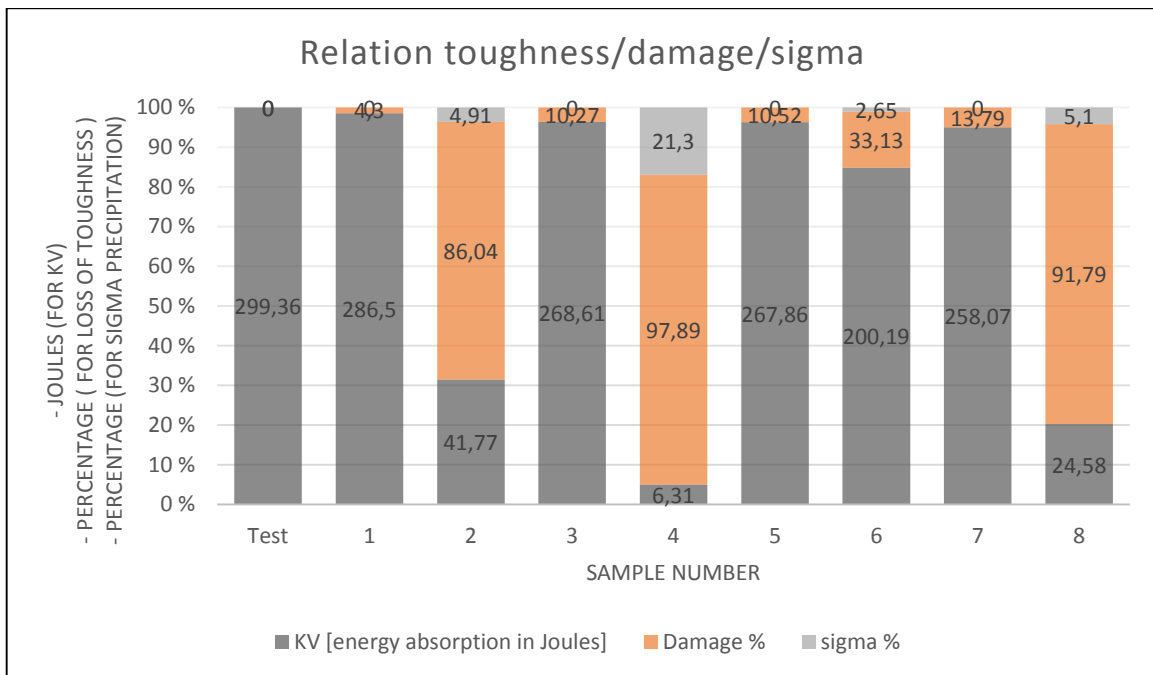


Figure 23-Individual relation between toughness, percentage of damage and percentage of sigma phase

Figure 23 shows the relation between alloys toughness (in terms of KV “toughness” measured in Joules), the calculated damage and the amount of σ phase (both in percentage).

RESULTS

Odd number samples present no sign of σ precipitation and the apparent loss of energy absorption is due to chrome nitride precipitation in the ferrite grains.

Even number present samples with different stages of σ precipitation, explaining the loss of toughness and the high percentage of damage.

RESULTS

4.2. UNS S31254 – SUPER AUSTENITE STAINLESS STEEL

METALLOGRAPHIC EVALUATION

HOLDING TIME 12 MINUTES – TEMPERATURE RANGE 1000°C - 600°C

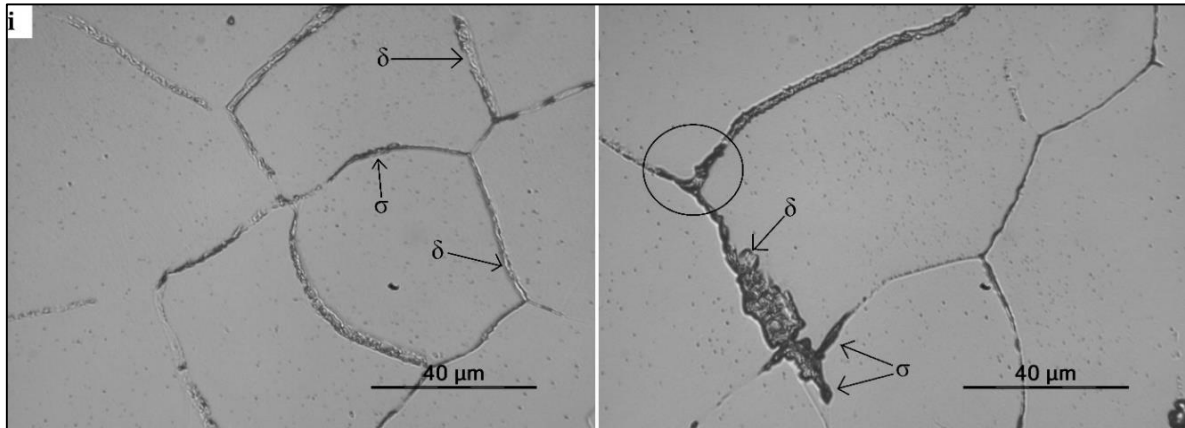


Figure 24-Sample 2. Two regions of the microstructure after 12 minutes holding time

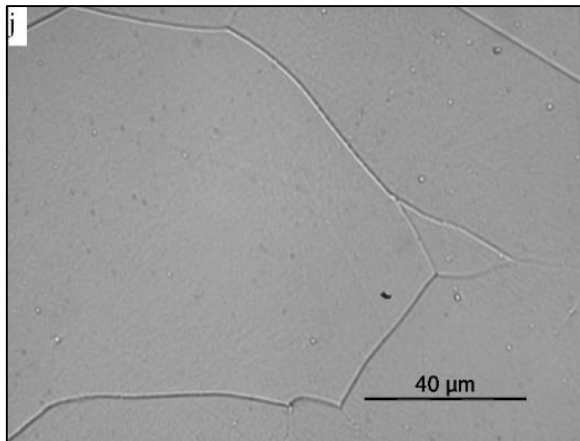


Figure 25-Sample 1 after HT1 and HT5. No sign of secondary phases.

Precipitation of σ is visible in δ/γ phase boundaries. One situation, shown in the second illustration (fig. 24), has a severe nucleation of σ , apparently initiated at a triple junction.

Bright color in the boundaries are signs of δ ferrite.

The result after the correct heat treatment is presented in figure 25 showing a good rearrangement of the grains, free for any form of detrimental phase.

RESULTS

HOLDING TIME 23 MINUTES – TEMPERATURE RANGE 1000°C - 600°C

Prolongation of holding time up to 23 minutes shows a progression of precipitation. Boundaries in figure 30 show greater propagation of δ ferrite and further precipitation of σ phase.

After the correct heat treatment, microstructure is free for any detrimental phase.

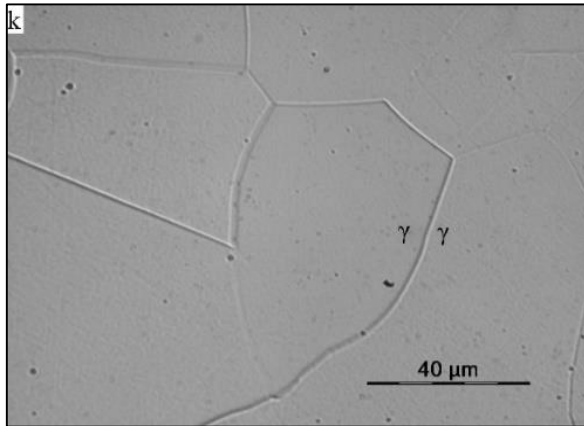


Figure 26-Sample 3 after HT2 and HT5. No sign of secondary phases

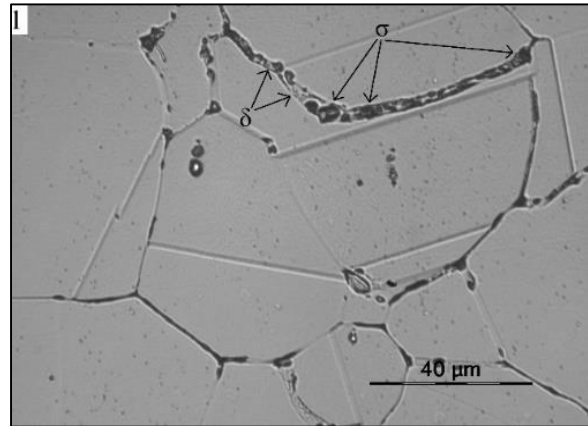


Figure 27-Sample 4. Highlighted region with a consistent precipitation of secondary phases

RESULTS

HOLDING TIME 6 MINUTES – TEMPERATURE RANGE 1000°C - 600°C

In figure 28 small tendencies of nucleation in δ/γ boundaries are visible.

Figure 29 is the result after proper heat treatment (HT5). The highlighted region shows a small area of the microstructure where precipitation of σ has remained along grain boundaries.

This result was unexpected. Region must have been subjected to an undesired heat treatment over a longer period where grain boundaries were Cr depleted and precipitated σ phase.

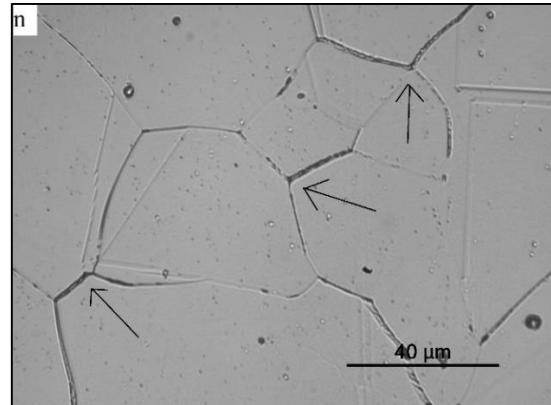


Figure 28-Sample 8 after HT4

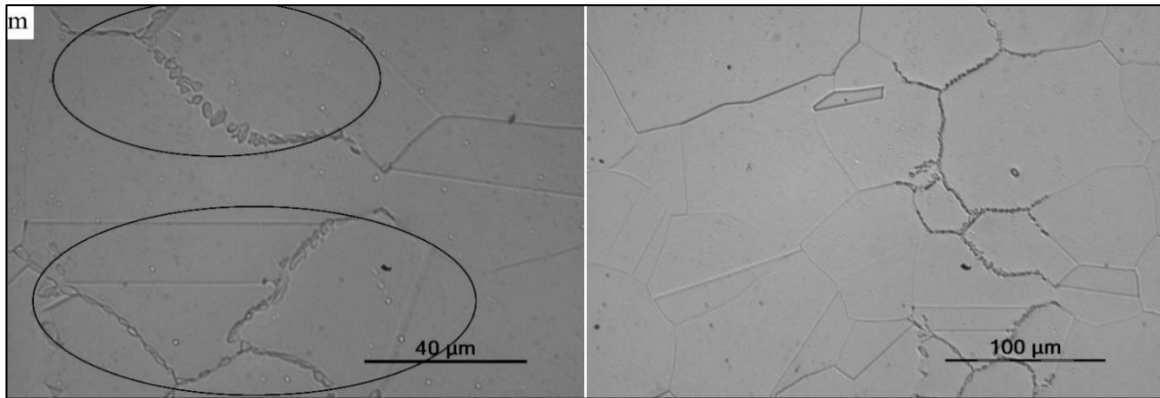


Figure 29-Sample 7 after HT4 and HT5

For heat treatment 3, where holding time was set to 1.2 minutes, no sign of detrimental phases appeared.

RESULTS

OBSERVATIONS

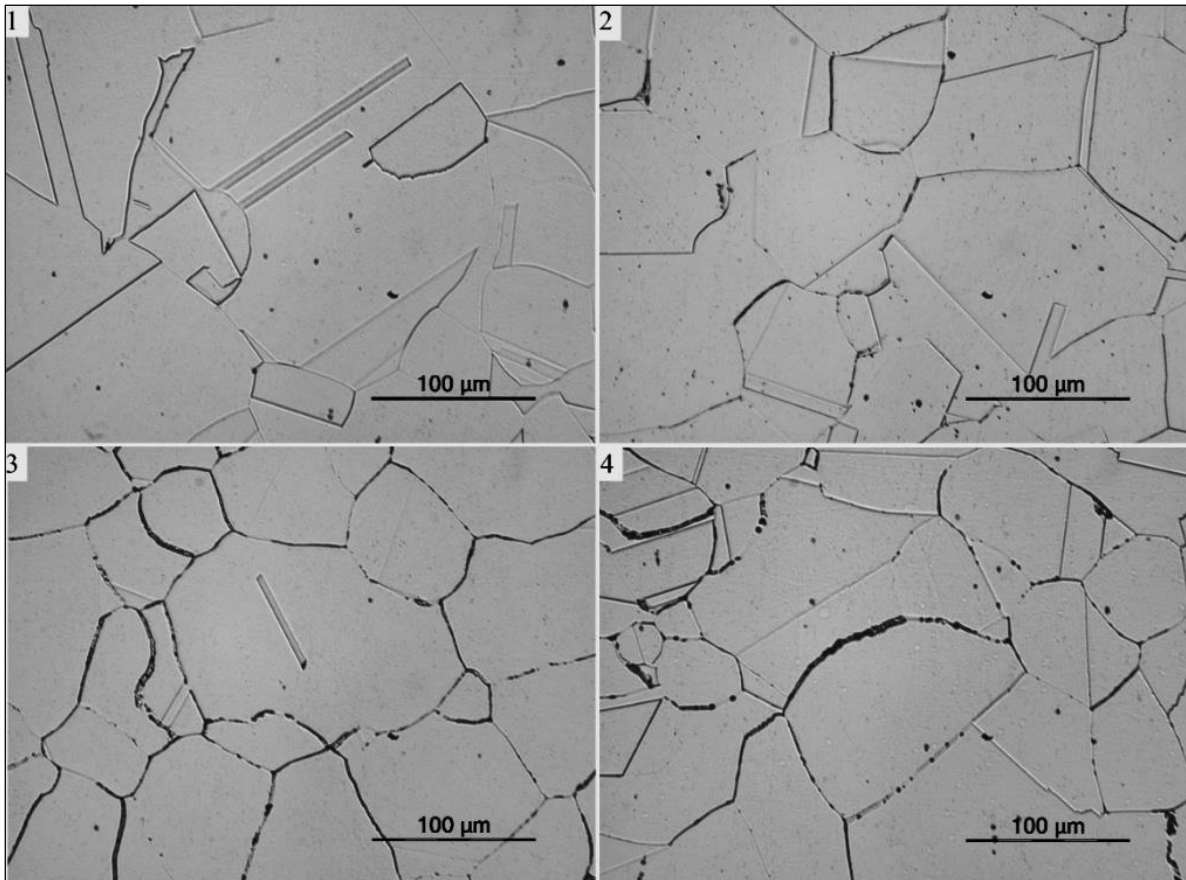


Figure 30--Precipitation in relation with holding time. 1)Holding time 1,2min 2)Holding time 6min 3)Holding time 12min 4)Holding time 23min.

Figure 30 shows the precipitation of σ when increased holding time (from 1 minute to 23 minutes). δ ferrite is located in the boundaries of δ/γ and appears as “thin” black boundary lines. As the holding time increases, σ phase precipitates in the Cr-rich boundaries and appears as “bold” black irregular lines.

After correct heat treatment, solution anneal temperature for 30 minutes and rapidly cooled in water, samples 1, 3 and 5 show good similarity to the initial microstructure free for σ phase. Only one scenario, sample 7 (fig. 29), precipitated σ in a specific region.

RESULTS

4.3. UNCERTAINTIES AND ERRORS

During research, some uncertainties regarding procedures and analysis appeared.

Systematic error of temperature adjustment for the furnace appeared. Accuracy of the furnace was studied and had a deviation of 3,5%. In solution anneal temperature, mentioned deviation equals to 40°C. For further measuring, a thermocouple data logger tracked temperature variations.

Cooling of samples is a source for random errors. Even procedure is defined, human handcraft was necessary to proceed. Variations in samples subjected to fast cooling were present. During this procedure, cooling happens in matter of seconds and small variations in performance can result in variances.

One situation (sample 7 UNS s31254 fig. 29), σ phase precipitated in grain boundaries. Taking to account kinetics theory and comparing it to other samples subjected to the same treatment, there is no logical reason that explains the outcome. A degree of uncertainty behind thermal treatment is present, where sample has been negatively affected.

Another particular source of error is machining of the materials.

Process includes milling and cutting, where tensile stresses and wear of the surface can result in energy transformed into heat. During execution, coolant is occasionally applied manually to dissipate heat. Wrong or inconsistent spreading of the liquid can result in an early undesired heat treatment of the sample.

In this research, an error during machining samples for Charpy test was done. Samples were taken out in the longitudinal direction to the rolling direction. A difference in grain orientation of the transverse direction was neglected. Discrepancies of the results were a consequence of this mistake. An average factor between the transverse grain orientations was calculated to adjust the results. Approach is explained in Appendix A.

DISCUSSION

5. DISCUSSION

As an overall observation, the behavior of both materials is clear. Increase of the holding time in the 1000 °C to 600 °C range increases the precipitation of σ phase.

Charpy test was performed on all samples from UNS S32760 super duplex alloy. The micrographs (fig. to fig.) show two distinct behaviors.

For the samples subjected to only a detrimental heat treatment (even number samples), different stages of σ precipitation were present. The worst case revealed more than 20% of σ between α - and γ -grains and resulted in a loss of toughness of 97,89%. Even lesser amounts of σ revealed a drastic drop in the ductile behavior of the alloy.

The samples subjected to a two stage heat treatment (first a heat treatment with a negative effect and then a final heat treatment rapidly cooled), marked with odd numbers, had no sign of previous σ precipitation. Precipitation of Cr_2N appeared in all samples subjected to a fast cooling in the middle of thick ferrite grains. The ductility of the material increased to acceptable levels, presenting a loss of toughness to a maximum of 13,79%.

UNS S31254 super austenite alloy was subjected to the exact same heat treatments.

Super austenite stainless steel is mainly composed by austenite grains. Since precipitation of σ phase has a higher diffusion velocity (about 100 times) in δ ferrite than γ austenite, all samples subjected to only a detrimental heat treatment showed only precipitation of secondary phases in grain boundaries.

Three out of four samples subjected to a two stage heat treatment showed a complete rearrangement of the microstructure. Previous detrimental phases were not present. One situation showed what is truly believed a nucleation of σ precipitates along the grain boundaries. This phase was only visible in a small region of the studied micrograph and the source is believed to come from a failure during quenching.

While some progression has been made throughout this research in the development of a recovery procedure for stainless steel affected by σ phase, the improvement of this study and considerably more work are needed to understand the behavior and properties of rehabilitated stainless steel.

The procedure chosen for provoking σ phase should be improved. In this research a continuous cooling over different periods of time was a poor decision of mine. The formation ratio of sigma phase is highest around 800 °C. With temperature as a variable, the formation ratio was not fixed, making it difficult to determine a total amount of secondary phase. A thermal treatment based on a fixed temperature and holding time as a variable will clarify the task, simplifying a future retry of the assignment.

Toughness was only measured on duplex steel and corroborated the effect of σ phase. It is believed that ductile-to-brittle transition has a lack of effect on the FCC structure in austenitic steel. Still, it would be of interest to compare the behavior of the alloy before and after being rehabilitated.

In this research only light optical microscope has been used to assess the microstructure of the sample. Diffraction analysis through scanning- or transmission- electron microscopy is preferred when determining secondary phases.

The theory behind stainless steel kinetics showed good accordance with results. Many studies confirm the negative effect of σ in corrosive environments (16) (17). As a natural progression, corrosion analysis of the previous damaged material and the rehabilitated material are recommended. All samples collected during this research are delivered to the supervisor in question.

Overall positive results from each analysis could in theory be interpreted as the possibility to implement a «recovery procedure» on materials being in service. Further research should be taken full scale, continued by a risk assessment of execution on in-service structures.

CONCLUSION

6. CONCLUSION

In this study two high alloy stainless steels have been evaluated.

Super duplex stainless steel shows larger propensity to formation of detrimental phases, such as σ phase and χ phase, compared to super austenite stainless steel.

Direct precipitation of σ phase in ferrite phase is in general fast. The main reason is that σ phase forming elements, such as Cr, Mo and Si, found in the alloys diffuse 100 times faster in ferrite phase than austenite. Then, Duplex stainless steel, with approximately 50% ferrite phase in its stable solution, has a higher precipitation level than stainless steel with fully austenitic microstructure.

Alloys were submitted to light optical microscopic evaluation and both showed good restructuration during correct thermal heat treatment, after being exposed to precipitation of detrimental phases.

In the majority of the situations the samples dissolved all previous detrimental phases in solution anneal temperature.

Duplex stainless steel experienced Chrome nitride-precipitation in all samples where rapidly cooling was applied.

Super austenitic stainless steel had initially lower percentage of detrimental phases. After thermal treatment where rapid cooling was present, one out of four samples experienced σ phase precipitation in one specific region of the grain boundaries. It is believed to be a result from wrong machining or a poor performance during thermal treatment.

Toughness was only evaluated on super duplex stainless steel.

Increasing amount of σ phase has an exponential deteriorating effect on ductility. A complete transition from ductile to brittle behavior is achieved with 20% σ phase.

Correct thermal treatment shows a beneficial recovery of toughness, increasing ductility up to a good level.

REFERENCES

REFERENCES

1. **Chater, James.** *Mount everest in the sea.* 2007. pp. 1-5.
2. **Bernhardsson and Charles.** *Duplex stainless steels '91.* s.l. : Les editions de physique, 1991.
3. **Cobb, Harold M.** *The history of Stainless Steel.* s.l. : ASM International, 2010.
4. **Chater, James.** Duplex stainless: challenges and opportunities. *www.kcicms.com.* [Online] 2012.
http://www.kcicms.com/pdf/factfiles/duplex/ssw1206_duplex_kci.pdf?resourceId=417.
5. **Forum, International Stainless Steel.** *www.worldstainless.org.*
www.worldstainless.org. [Online] may 4, 2012.
<http://www.worldstainless.org/news/show/90>.
6. **Khatak and Raj, Baldev.** *Corrosion of austenitic steels.* Kalpakkam : Woodhead publishing limited, 2002. 1-84265-100-5.
7. **The international molybdenum association, IMOA.** *Practical guidelines for the fabrication of Duplex Stainless steels.* 2014. pp. 8 - 10.
8. **French, David.** <http://www.nationalboard.org/>.
<http://www.nationalboard.org/index.aspx?pageID=164&ID=192>. [Online] winter 1992.
<http://www.nationalboard.org/index.aspx?pageID=164&ID=192>.
9. **Gunn, Robert.** *Duplex stainless steels.* s.l. : Abington publishing, 1997.
10. **Pohl, Michael, Storz, Oliver and Glogowski, Thomas.** *Effect of intermetallic precipitations on the properties of duplex stainless steel.* s.l. : Elsevier, 2005.
11. **Kovach, Curtis.** *High performance stainless steels.* Pittsburgh : Parr, 2011.
12. **Charles, J. and Bernhardsson, S.** *Duplex stainless steels.* Borgougne : les editions de physique, 1991.
13. **D.M.Escriba.** *Chi-phase precipitation in a DSS.* São Paulo : Elsevier, 2009.
14. **Hereñu, S.** *The influence of chromium nitrides precipitation on the fatigue behaviour of DSS.* Argentina : Elsevier, 2014.
15. **Sieurin, Henrik.** *Fracture toughness properties of duplex stainless steels.* Stockholm : Royal Institute of Technology, 2006.
16. **Féron.** *Marine corrosion of stainless steels.* London : IOM Communications, 2001.
17. **Magnabosco, Rodrigo.** *Kinetics of sigma phase formation in a DUplex Stainless Steel.* São Bernardo do Campo : SCIELO, 2009. 1980-5373.

REFERENCES

18. **Statoil.** *Metallographic etching of duplex stainless steels.* 2010. pp. 3-9.
19. **Hsieh, Chih-Chun and Wu, Weite.** Overview of Intermetallic Sigma Phase Precipitation in Stainless Steel. *Hindawi publishing corporation.* [Online] 1 1, 2012. [Cited: 4 1, 2015.] <http://www.hindawi.com/journals/isrn/2012/732471/>.
20. **Villanueva, D.M.E., et al.** *Comparative study on sigma phase precipitation of three types of stainless steels: austenitic, superferritic and duplex.* s.l. : Maney, 2006.
21. **Smuk, Olena.** *Microstructure and properties of modern P/M super duplex stainless steels.* Stockholm : Royal Insitute of Technology, 2004. 91-7283-761-6.
22. **American Society for testing and Materials, ASTM.** *A370 - 08a.* s.l. : ASTM, 2008.
23. **Statoil.** *Metallographic etching of duplex stainless steel.* 2010.
24. **G.K.Narula, K.S.Narula and V.K.Gupta.** *Materials Science.* s.l. : Tata McGraw-Hill, 1988. 0-07-451796-1.

APPENDIX

APPENDIX

- A. Charpy V-notch impact test clarification and results. (2 pages)
- B. Calculations regarding theoretical approach for cooling ratio and experimental data for cooling processes (2 pages)
- C. MDS 630 – NORSOK's Material data sheet for UNS s32760 and UNS s31254 (3 pages)
- D. Certification UNS S32760 (2 pages)
- E. Certification UNS S31254 (2 pages)
- F. Schematic representation of sigma phase precipitation (2 pages)
- G. Equipment
- H. Organization of samples for further studies

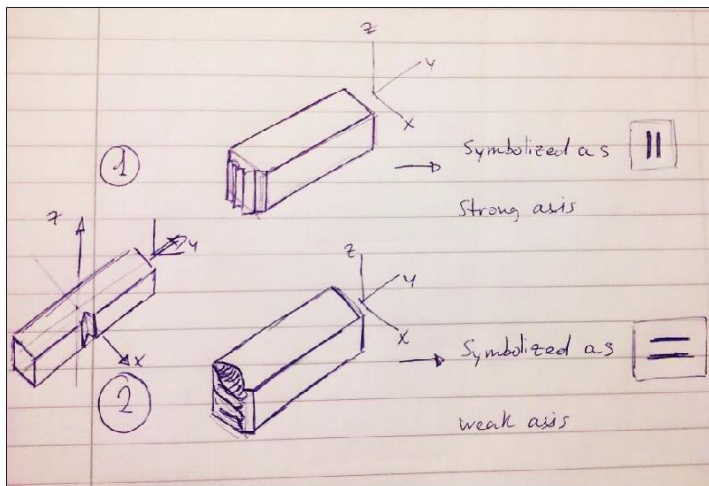
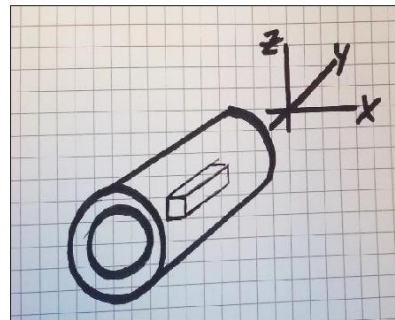
APPENDIX

APPENDIX A. CHARPY V-NOTCH IMPACT TEST CLARIFICATION AND RESULTS

Information

Calibration	ISO 13802
Maximum impact force	450 J
Raised Angle	149,9 deg
Sample temperature	-46 deg celsius

When producing samples for Charpy test, grain direction has a major influence in the results. For this research, longitudinal axis were selected (read y-axis). As a misunderstanding, Z-X direction wasn't taken to account. This resulted in discrepancies in the results.



As a correction for the error made, a relation factor was found between Z and X axis. Grain direction appeared when examining fracture (shown in figure). By dividing results after axis, a relation factor between strong- and weak-axis was found. This factor has been used to normalize all results and calculate the average value. Values marked as green or yellow, are original results depending on the grain direction of the samples. Values in red are based on the ratio number.

Ratio	0,65
-------	------

APPENDIX

Test piece	Result [J]	Avg [J]	Failure type	Grain dir.	Test p.	Results [J]	Avg [J]	Failure type	Grain dir.
T1	309,71	299,36	Hinge	1					
T2	285,71	194,58	Hinge	1					
T3	302,65		Hinge	1					
2.1	27,52	41,77	Rupture	2	1.1	283,9	286,50	Hinge	1
2.2	22,94	27,15	Rupture	2	1.2	160,89	160,89	Hinge	2
2.3	30,99		Rupture	2	1.3	289,1		Hinge	1
4.1	6,31	6,31	Rupture	1	3.1	168,82	268,61	Hinge	2
4.2	4,32	4,12	Rupture	2	3.2	268,61	167,53	Hinge	1
4.3	3,91		Rupture	2	3.3	166,24		Hinge	2
6.1	189,88	200,19	Hinge	2	5.1	175,25	267,86	Hinge	2
6.2	191,7	189,88	Hinge	1	5.2	264,7	175,25	Hinge	1
6.3	208,67		Hinge	1	5.3	271,02		Hinge	1
8.1	27,01	24,58	Rupture	1	7.1	248,07	258,07	Hinge	1
8.2	25,81	15,97	Rupture	1	7.2	250,16	167,75	Hinge	1
8.3	20,91		Rupture	1	7.3	275,98		Hinge	1

Information

Grain direction	1 stand for strong axis, the one used for further evaluation 2 stands for weak axis
Failure type	Hinge stands for partial break. More ductile than brittle. Rupture stands for complete break. More brittle than ductile.
Values	Based on average of three. Green box shows value of strong axis. Yellow box shows value of weak axis. If box is colored red, means it's based on the other axis and the relation factor.

APPENDIX

APPENDIX B. CALCULATIONS REGARDING THEORETICAL APPROACH FOR COOLING RATIO AND EXPERIMENTAL DATA FOR COOLING PROCESSES

Temperature drop - air medium

Stephan-Boltzmann law - Formula

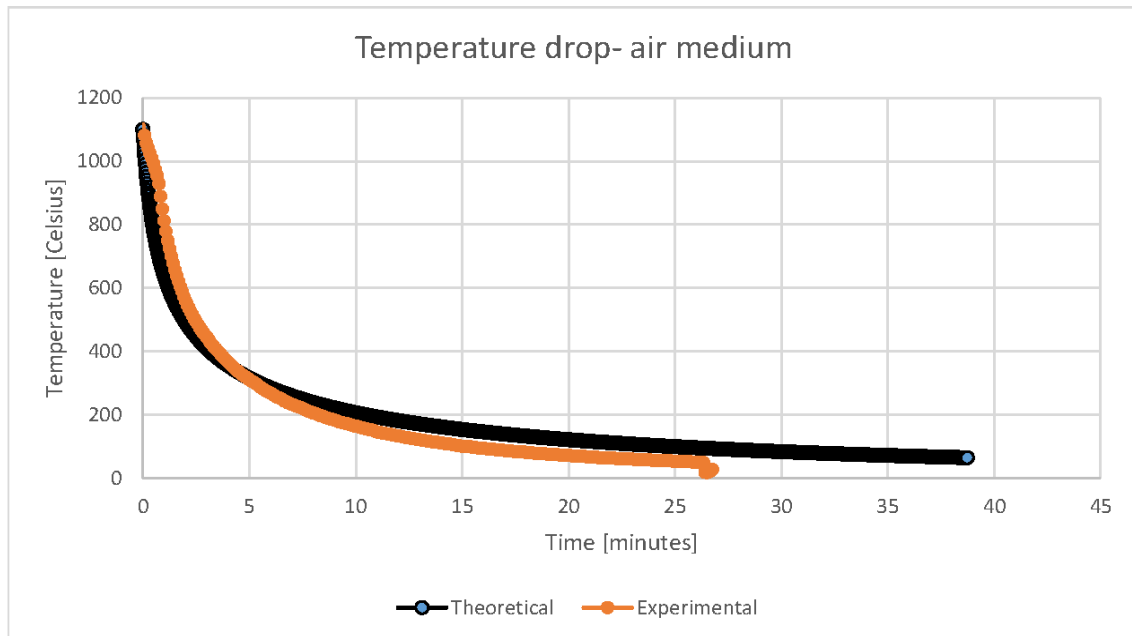
$$P = A \cdot \varepsilon \cdot \sigma \cdot T^4$$

$$T_{drop} = \frac{(P \cdot t)}{(m \cdot c_{steel})}$$

where:

- T T_material-T_environment
- ε Black body
- σ Constant of proportionality
- A Surface area of material
- m Steel mass
- c_steel Heat capacity of steel

Input data	Unit		
Surface Area steel	A	0,003168	m ²
Temp. Material	T_mat	1393	K
Black body	ε	1	unitless
Prop. Constant	σ	5,67E-08	W/m ² *K
Temp. Environm.	T_env	293	K
steel mass	m	0,07	kg
heat cap. Steel	c_steel	500	J/kg*K



APPENDIX

Temperature drop - water medium

Newton's law of Cooling - Formula

$$T(t) = T_{env} + C \cdot e^{-k \cdot t}$$

where:

T_{env} Temperature environment
 C Difference Initial temp. and environment
 k thermal conductivity
 t time

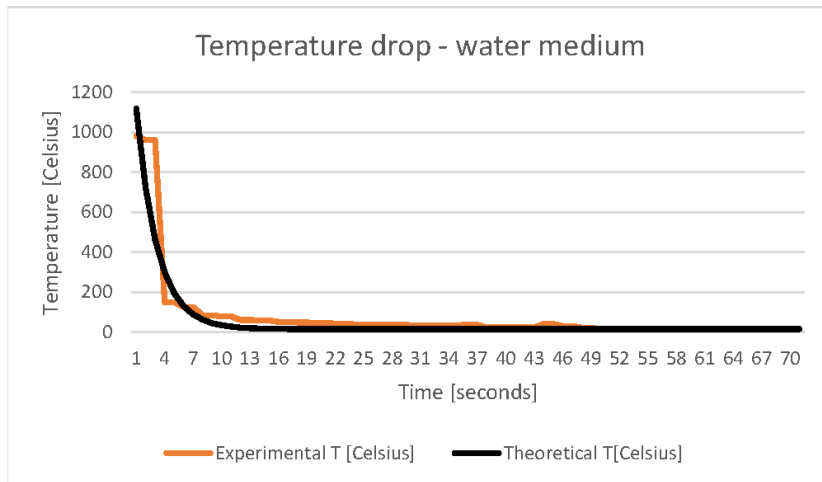
Thermal conductivity - Equation

$$k = \frac{(h \cdot A)}{(m \cdot c_{steel})}$$

where:

h Heat coefficient of water
 A Surface Area of material
 m Mass of material
 c_{steel} Heat capacity of steel

Input data		Unit	
Surface Area steel	A	0,003168	m ²
Heat coef. Water	h	5000	W/m ² *K
steel mass	m	0,07	kg
heat cap. Steel	c _{steel}	500	J/kg*K
Temp. Environm.	T _{env}	15	C
Diff. Temp.	C	1105	C
heat cap. water	c _{water}	4180	J/kg*K
thermal conductivity	k=hA/mc	0,452571	W/mK



To decide amount of water, I calculate the Ratio water mass/steel mass

$$\frac{m_w}{m_s} = \frac{c_{steel}}{c_{water}} \cdot \frac{T_{start} - T_{end}}{T_{end} - T_{envr}}$$

Water/Steel-R

4,349152

APPENDIX

APPENDIX C. MDS 630 – NORSOK’S MATERIAL DATA SHEET FOR UNS S32760 AND UNS S31254

NORSOK Standard

MATERIAL DATA SHEET		MDS D51		Rev. 3
<i>TYPE OF MATERIAL:</i> Ferritic / Austenitic Stainless Steel, Type 25Cr duplex				Page 1 of 2
<i>PRODUCT</i>	<i>STANDARD</i>	<i>GRADE</i>	<i>ACCEPT. CLASS</i>	<i>SUPPL. REQ.</i>
Seamless pipes	ASTM A 790	UNS S 32550 UNS S 32750 UNS S 32760	-	-
<i>1. SCOPE</i>	This MDS specifies the selected options in the referred standard and additional requirements which shall be added or supersede the corresponding requirements in the referred standard. This MDS is based on the mechanical properties of UNS S 32750.			
<i>2. QUALIFICATION</i>	Manufacturers of product to this MDS shall comply with the requirement of NORSOK Standard M-650.			
<i>3. STEEL MAKING</i>	The steel melt shall be refined with AOD or equivalent.			
<i>4. HEAT TREATMENT</i>	The pipes shall be solution annealed followed by water quenching.			
<i>5. CHEMICAL COMPOSITION</i>	PRE = % Cr + 3.3 % Mo + 16 % N ≥ 40.0			
<i>6. TENSILE TESTING</i>	R _{p0.2} ≥ 550 MPa; R _m ≥ 800 MPa; A ₅ ≥ 25%			
<i>7. HARDNESS</i>	The harness shall be max. 32 HRC (or alternatively 301 HB or 330 HV 10).			
<i>8. IMPACT TESTING</i>	Charpy V-notch testing according to ASTM A 370 at - 46 °C is required for thickness ≥ 6 mm. The minimum absorbed energy shall be 45 J average / 35 J single. Reduction factors for sub-size specimens shall be: 7.5 mm - 5/6 and 5 mm - 2/3.			
<i>9. CORROSION TEST</i>	Corrosion test according to ASTM G 48 Method A is required. Test temperature shall be 50 °C and the exposure time 24 hours. The specimen shall have the internal and external surfaces in the as-delivered condition (including pickling). Cut edges shall be prepared according to ASTM G 48, and the whole specimen shall be pickled (20 % HNO ₃ + 5 % HF, 60 °C, 5 minute). The test shall expose the external and internal surfaces and a cross section surface in full wall thickness. The acceptance criteria are: - No pitting 20 X magnification. - The weight loss shall be less than 4.0 g/m ² .			
<i>10. MICROGRAPHIC EXAMINATION</i>	The micrographic examination shall cover the near surfaces and mid-thickness region of the pipe. The ferrite content shall be determined according to ASTM E 562 or equivalent and shall be within 35-55 %. The microstructure, as examined at 400 X magnification on a suitably etched specimen, shall be free from intermetallic phases and precipitates.			
<i>11. EXTENT OF TESTING</i>	Charpy V-notch impact, microstructure, hardness, corrosion and tensile testing shall be carried out for each lot as defined in the referred standard. For batch furnace charges the specified tests shall be carried out for each heat treatment charge.			
<i>12. TEST SAMPLING</i>	Samples for production testing shall realistically reflect the properties in the actual components.			
<i>13. SURFACE FINISH</i>	White pickled.			
<i>14. REPAIR OF DEFECTS</i>	Weld repair is not acceptable.			

APPENDIX

NORSOK Standard

MATERIAL DATA SHEET		MDS D51	Rev. 3	
<i>TYPE OF MATERIAL:</i> Ferritic / Austenitic Stainless Steel, Type 25Cr duplex			Page 2 of 2	
<i>PRODUCT</i>	<i>STANDARD</i>	<i>GRADE</i>	<i>ACCEPT. CLASS</i>	<i>SUPPL. REQ.</i>
Seamless pipes	ASTM A 790	UNS S 32550 UNS S 32750 UNS S 32760	-	-
<i>15. MARKING</i>	The component shall be marked to ensure full traceability to melt and heat treatment lot.			
<i>16. CERTIFICATION</i>	<p>Certification shall affirm compliance with the specification and shall be according to EN 10204 Type 3.1B provided the manufacturer has a quality assurance system certified by a competent body established within the EC, and having undergone a specific assessment for materials.</p> <p>Heat treatment temperature, soaking time and cooling medium should be stated in the certificate.</p>			

APPENDIX

NORSOK Standard

MATERIAL DATA SHEET		MDS R11		Rev. 3
<i>TYPE OF MATERIAL:</i> Austenitic stainless steel, Type 6Mo				Page 1 of 1
<i>PRODUCT</i>	<i>STANDARD</i>	<i>GRADE</i>	<i>ACCEPT. CLASS</i>	<i>SUPPL. REQ.</i>
Seamless pipes	ASTM A 312	UNS S31254 UNS N08367 UNS N08926	-	-
<i>1. SCOPE</i>	This MDS specifies the selected options in the referred standard and additional requirements which shall be added or supersede the corresponding requirements in the referred standard.			
<i>2. QUALIFICATION</i>	Manufacturers of product to this MDS shall comply with the requirement of NORSOK Standard M-650.			
<i>3. STEEL MAKING</i>	The steel melt shall be refined by AOD or equivalent.			
<i>4. HEAT TREATMENT</i>	The pipes shall be solution annealed followed by water quenching.			
<i>5. TENSILE TESTING</i>	$R_{p0.2} \geq 310$ MPa, $R_M \geq 675$ MPa for $t \leq 5.0$ mm and $R_M \geq 655$ MPa for $t > 5.0$ mm, $A_5 \geq 35$ % (long.)			
<i>6. CORROSION TESTING</i>	Corrosion test according to ASTM G 48 Method A is required. Test temperature shall be 50 °C and the exposure time 24 hours. Test specimens shall have the internal and external surfaces in the as-delivered condition (including pickling). Cut edges shall be prepared according to ASTM G48, and the whole specimen shall be pickled (20 % HNO ₃ + 5 % HF, 60 °C, 5 minute). The test shall expose the external and internal surfaces and a cross section surface in full wall thickness. The acceptance criteria are: <ul style="list-style-type: none"> - No pitting at 20 X magnification. - The weight loss shall be less than 4.0 g/m. 			
<i>7. EXTENT OF TESTING</i>	Corrosion test shall be carried out to the same extent as stated for mechanical tests in the referred standard.			
<i>8. TEST SAMPLING</i>	Samples for production testing shall realistically reflect the properties in the actual components.			
<i>9. SURFACE FINISH</i>	White pickled.			
<i>10. REPAIR OF DEFECTS</i>	Weld repair is not acceptable.			
<i>11. MARKING</i>	The component shall be marked to ensure full traceability to melt and heat treatment lot.			
<i>12. CERTIFICATION</i>	Certification shall affirm compliance with the specification and shall be according to EN 10204 Type 3.1B provided the manufacturer has a quality assurance system certified by a competent body established within the EC, and having undergone a specific assessment for materials. Heat treatment temperature, soaking time and cooling medium should be stated in the certificate.			

APPENDIX

APPENDIX D. INSPECTION CERTIFICATE UNS S32760



T.T.I. - Tubacex Tubos Inoxidables, S.A.

Registro Mercantil de Alava, Tomo 587, Folio 189, Hoja VI 2885 - N.I.F. A-01140227

Printed on:
01.02.2008

INSPECTION CERTIFICATE EN 10204 3.1	Number: [REDACTED]	Rev: 0
	Page: 1 / 2	
Date: 01.02.2008		01.02.2008

CUSTOMER : [REDACTED]
 STANDARD : ASTM-A 790M-05B
 ADDIT. SPECS : MDS: SFF-D51 REV.1 + NACE MR01.75-03
 GRADE : UNS S32760
 DIMENSIONS : 6" SCH 120
 MATERIAL : SEAMLESS STAINLESS STEEL TUBE
 HOT FINISHED; PASSIVATED;
 PLAIN BEVELLED ENDS;

U: 052183

YOUR	ITEM	T.T.I.	HEAT NR.	NO. OF PIECES	WEIGHT KG	TOTAL LENGTH	UNIT LENGTH--
		4	39209	1	274	5,00	5 - 7 MT

RAW MATERIAL
 MELTING PROCESS: ELECTRIC FURNACE + A.O.D FROM: ACERALAVA
 PEELED BARS; MACROETCH TESTING: GOOD;

CHEMICAL COMPOSITION (*1 L: LADLE; C: PRODUCT *7 PRE)

*1 HEAT	C	Mn	Si	P	S	Ni	Cr	Mo	Cu	W	N	*7
L 39209	0,018	0,68	0,510	0,024	0,0004	6,95	25,50	3,66	0,68	0,560	0,2415	41,442

HEAT TREATMENT
 SOLUTION ANNEALED 1110 °C RAPIDLY COOLED

HEAT NR.	TEST	T(°C)	RM	MPA	RP	%	Z	%JULIOS	CHARPY 2V	10 * 10	HRC
39209	712079	20	831,0	577,0	693,0	40,0		-46	172,0	182,0	24 25

TECHNOLOGICALS
 FLATTENING TEST: GOOD

METALLURGICAL TEST
 STRUCTURE FREE FROM INTERMETALLIC PHASES AND PRECIPITATES
 INTERGRANULAR CORROSION: A-262 PRACT."E": NOT OBJECTIONS

FERRITE CONTENT AS PER ASTM E562

HEAT	ITEM	%FERRITE	+/-
39209	000004	53,70	1,7

CHECKED BY: *Jaw*
 SITAS Q.C-DEPT.

NON DESTRUCTIVE TEST
 100 % HYDROSTATIC PRESSURE TESTED AT 196 BAR , DURING 5 SEC, GOOD
 STEEL GRADE CHECKING ON EACH TUBE BY SPECTROMETRY (PMI)
 DIMENSIONAL CHECKING ON EACH TUBE, SATISFACTORY
 VISUAL INSPECTION ON EACH TUBE, SATISFACTORY

MARKS
 TUBACEX ASTM-A 790 UNS S32760 6" SCH 120 SMLS HEAT/..... PMI

REMARKS
 - PITTING CORROSION TEST AT 50°C/24 HOURS ACC. TO ASTM G-48 METHOD "A":
 NO PITTING OBSERVED AT 20X MAG.
 WEIGHT LOSS: 0 G/M2.

NO WELD REPAIR WAS PERFORMED
 MATERIAL MANUFACTURER APPROVED WITH CERTIFICATE NR. 07/2001/MUC BY TÜV SÜDDEUTSCHLAND (NOTIFIED BODY 0036) TO ISSUE CERTIFICATES OF SPECIFIC PRODUCT CONTROL IN ACCORDANCE WITH PRESSURE EQUIPMENT DIRECTIVE 97/23/EC ANNEX 1 POINT 4.3.
 MATERIAL CHARACTERISTICS COMPLY WITH POINT 7.5 OF ANNEX I TO PED BY HAVING AN ELONGATION



We hereby certify that the material herein described has been manufactured, sampled, tested and inspected in accordance with above standards and specifications and satisfies the order's requirements.
 This certificate is issued by a computerized system and it is valid without original signature. In case the owner of the certificate would release a copy of it, he must attest its conformity to the issued, assuming the responsibility for any unlawful or T.T.I.S.A. not allowed use.
 Any forgery or falsification of this certificate shall legally prosecuted.

T.T.I.
 Tubacex Tubos Inoxidables, S.A.
 INGENIERIA DE CALIDAD

 Jon Altuna Zubizar

APPENDIX



T.T.I. - Tubacex Tubos Inoxidables, S.A.

Registro Mercantil de Alava, Tomo 587, Folio 188, Hoja VI 2885 - N.I.F. A-01140227

Printed on:
01.02.2008

INSPECTION CERTIFICATE
EN 10204 3.1

Number: [REDACTED]	Rev: 0
Page: 2 / 2	
Date: 01.02.2008	01.02.2008

CUSTOMER : [REDACTED]
 STANDARD : **ASTM-A 790M-05B**
 ADDIT.SPECS : **MDS: SFF-D51 REV.1 + NACE MR01.75-03**
 GRADE : **UNS S32760**
 DIMENSIONS : **6" SCH 120**
 MATERIAL : **SEAMLESS STAINLESS STEEL TUBE**
HOT FINISHED; PASSIVATED;
PLAIN BEVELLED ENDS;

AFTER RUPTURE AT TENSILE TEST NO LESS THAN 14 % AND A BENDING RUPTURE ENERGY AT IMPACT TEST NO LESS THAN 27 J AT 20°C.



We hereby certify that the material herein described has been manufactured, sampled, tested and inspected in accordance with above standards and specifications and satisfies the order's requirements.
 This certificate is issued by a computerized system and it is valid without original signature.
 In case the owner of the certificate would release a copy of it, he must attest its conformity to the issued, assuming the responsibility for any unlawful or T.T.I.,S.A. not allowed use.
 Any forgery or falsification of this certificate shall legally prosecuted.

T.T.I.
 Tubacex Tubos Inoxidables, S.A.
 INGENIERIA DE CALIDAD

 Jon Altuna Zubizarain

APPENDIX

APPENDIX E. INSPECTION CERTIFICATE UNS S31254



DMV STAINLESS France

B.P. 10 - F 21501 Montbard Cedex - FRANCE
 Tel : 33(0)3 80 89 52 00 Fax : 33(0)3 80 89 52 37
 Email : dmvfrance@dmv-stainless.com

No / Nr. / N°:

Page : 1 / 2

**INSPECTION CERTIFICATE
 ABNAHMEPRÜFZEUGNIS
 CERTIFICAT DE RECEPTION
 3-1-B - EN 10204: 1991 + A1:1997**

CUSTOMER / Kunde / Client : [REDACTED]
CUSTOMER'S PURCHASER ORDER [REDACTED]
DMV order no / DMV-Auftragsnr. / Commande DMV : [REDACTED]
DMV certified lot no / Zeugnis-Losnr. / Lot de certificat : [REDACTED]
Coming from / abgeteilt vom / venant de : Manufacturing lot no / Herstellungs-Losnr / Lot de fabrication [REDACTED]

Product :	Seamless stainless steel pipe or tube	Hot finished	Annealed	Pickled Passivated
Erzeugnis :	Nahtlose Stahlrohre	Warmgefertigt	Abgeschreckt	Gebeizt passiviert
Type de Produit :	Tubes sans soudure	Finis à chaud	Hypertrempés	Décapés Passivés

Grade(s) and Specification(s) / Stahlsorte und Liefervorschriften / Nuance(s) et spécification(s) :

UNS S31254
 ASTM A 312-03 + SPEC MDS SFF-R11 REV.7

Marking of the product / Kennzeichnung / Marquage :

DMV -F- ASTM A312 - UNS S31254 - 219.10 X 23.01 - 8" NPS X SCH 160 - HEAT : F02431 - SML - 21339302D - FRANCE -

Supplementary requirements / Zusätzliche Anforderungen / Prescriptions supplémentaires:

Size Tolerances / Abmessungstoleranzen / Tolérances Dimensionnelles : according to ASTM A 312-03

Pcs No	Weight	Total Length	OD	W.T	Min Length	Max Length
9	4063 Kg	35.822 m	219.10 mm 8" NPS	23.01 mm SCH 160	3338 mm	4089 mm

Chemical Analysis / Chemische Zusammensetzung / Caractéristiques Chimiques (%)

Melting Process / Erschmelzungsart / Elaboration : Electric/ Elektroshaf/ Electrique + AOD or VOD

Heat No / Schmelzen Nr. / N° Coulée : **F02431**

	C	Mn	P	S	Si	Ni	Cr	Mo	N	Cu
Min						17.5	19.5	6.00	0.18	0.50
Max	0.020	1.00	0.030	0.010	0.80	18.5	20.5	6.50	0.22	1.00
Heat/Schmelzen/Coulée	0.014	0.69	0.023	0.002	0.35	18.20	19.69	6.09	0.2110	0.69

Mechanical and Metallurgical Properties / Mechanische und Metallurgische Kennwerte / Caractéristiques Mécaniques et Métallurgiques

TENSILE TEST 20 °C		Y.S 0.2% (MPa)	Y.S 1% (MPa)	T. S (MPa)	Elongation (50.8 mm)
Zugfestigkeit	Requirements :	Min 300	Min 340	Min 650	Min 35
Traction	Results :	360	406	683	53.1

FLATTENING / RINGFALT / APLATISSEMENT :

N876 / N877 OK-o.B-Bon

HARDNESS TEST / HAERTE / DURETE :

N876 Requirements : <=35HRC <18

CORROSION / KORROSION / CORROSION :

N876 Requirements : ASTMG48 /50°C/24H OK-o.B-Bon (Weight Lost 0.02023 mg/cm²)

APPENDIX



DMV STAINLESS France

B.P. 10 - F 21501 Monthard Cedex - FRANCE
 Tel : 33(0)3 80 89 52 00 Fax : 33(0)3 80 89 52 37
 Email : dmvfrance@dmv-stainless.com

No / Nr. / N°:

Page : 2 / 2

**INSPECTION CERTIFICATE
 ABNAHMEPRÜFZEUGNIS
 CERTIFICAT DE RECEPTION
 3-1-B - EN 10204: 1991 + A1:1997**

DMV order no / DMV-Auftragsnr. / Commande DMV : [REDACTED]

Other testing and Declaration / Andere Versuche und Bemerkungen / Autres essais et Déclarations

- Visual and dimensional examination / Besichtigung und masskontrolle / Examen visuel et dimensionel : OK-o.B-Bon
- Hydrostatic Test / Wasserinnendruckversuch / Essai Hydraulique : 190 BARS / 5s
- Heat Treatment / Wärmebehandlung / Traitement Thermique : Température: 1150/1250°C
 Quenched in water / Lösungsgegluth und abgeschreckt / Hypertempé à l'eau.
- Antimixing checked by PMI / Prüfung auf Werkstoffverwechslung / Contrôle anti-mélange par PMI : OK-o.B-Bon
- No weld repair / Keine Reparaturschweissung / Aucune réparation par soudure.
- No contamination by mercury or mercury compounds / Keine Quecksilber - oder Quecksilberbestandteilkontamination
 Pas de contamination par le mercure ou l'un de ses composants.

*We certify that the delivered products comply with specification of the order.
 Die Erzeugnisse wurden bestellungsgemäss geprüft und für in Ordnung befunden.
 Nous attestons que les produits livrés sont conformes aux stipulations de la commande.*

Date d'édition :	07/02/2005	Contrôle Qualité :	Mme LARCHER
------------------	------------	--------------------	-------------

This certificate is issued by a computerized system and is valid without signature. On the original certificate, the DMV STAINLESS trade mark in blue color is stamped on the top left of the certificate. In case the corner of the original would release of a copy of it, he must attest its conformity for any unlawful or not allowed use. Any alteration and falsification will be subject to the law.

Dieses Zeugnis wurde mit Hilfe der EDV erstellt und ist ohne Unterschrift gültig. Links oben auf dem Originalzeugnis ist das DMV STAINLESS Warenzeichen in blauer Farbe gestempelt. Wenn der Besitzer des Originals eine Kopie erstellen würde, so müßte er die Übereinstimmung mit dem Original bestätigen lassen und hätte im Falle einer gesetzeswidrigen oder unerlaubten Verwendung die Verantwortung zu tragen. Jede un- oder Fälschung wird gerichtlich verfolgt.

Ce certificat a été préparé et édité par un système informatique et est valable sans signature. Les documents originaux informatiques sont identifiés par le logo DMV STAINLESS de couleur bleue en haut à gauche du certificat. Dans le cas où le possesseur de l'original en délivrerait une copie, il devra en attester la conformité et en endosser la responsabilité en cas d'usage illicite. Toute altération ou falsification ou serait susceptibles d'entraîner des poursuites légales.

Confirmation with reference to Pressure Equipment Directive 97/23/EC: The works operates a quality management system that has undergone a specific assessment for materials for pressure equipment and is certified by a competent body (TUV-CERT.No: 05/2005/MAN)

DMV STAINLESS France S.A. ISO9001 - LRQA N° 926478

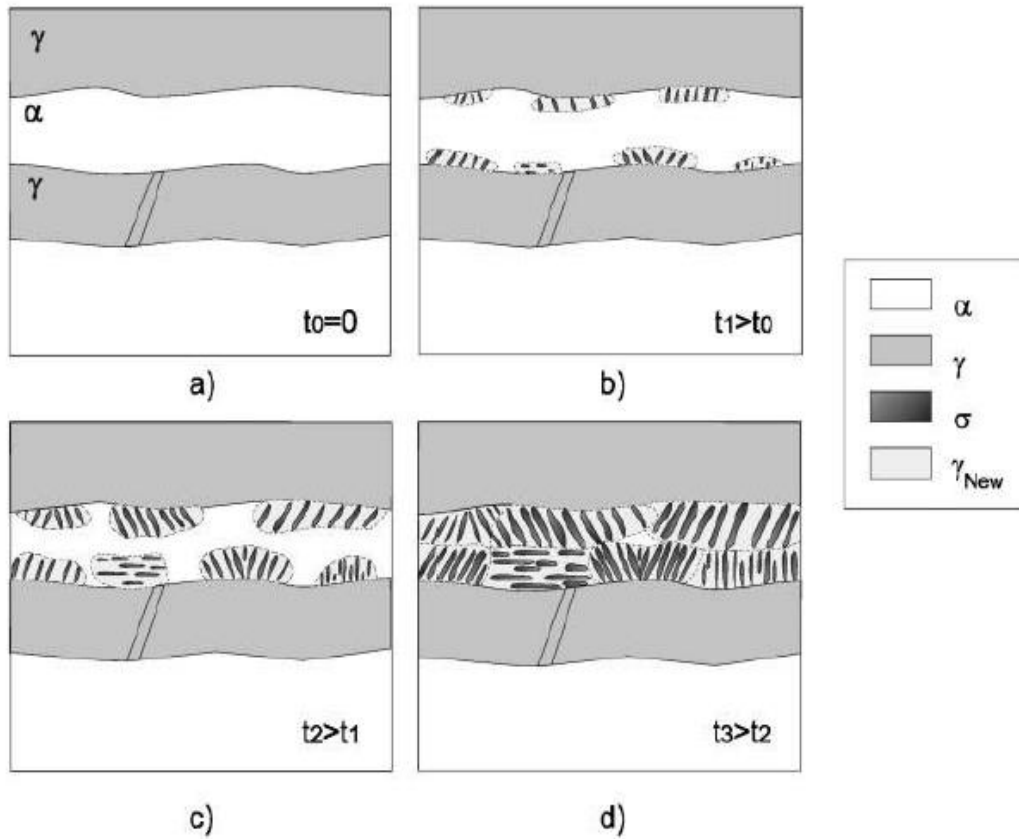


090.G0.051

APPENDIX

APPENDIX F. SCHEMATIC REPRESENTATION OF SIGMA PHASE PRECIPITATION

PRECIPITATION MECHANISM OF DUPLEX STAINLESS STEEL



Figures a-d show precipitation mechanism of σ in duplex stainless steel.

A) At service temperature, α and γ are free for secondary phases.

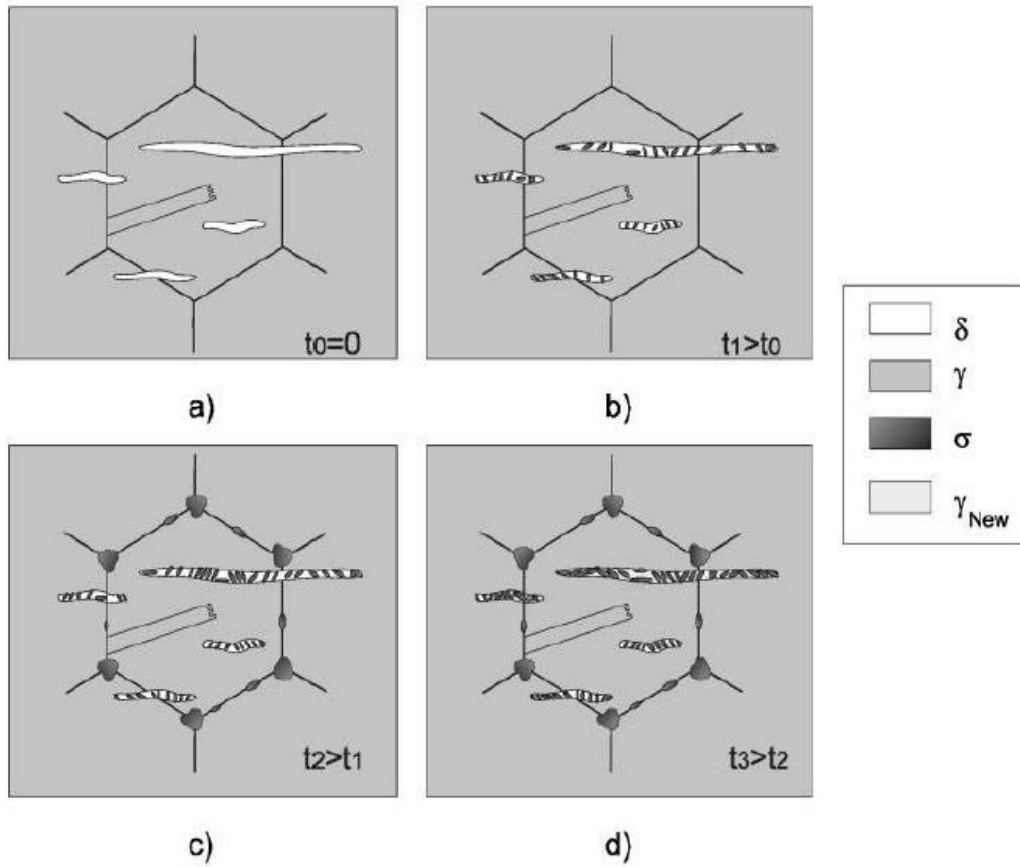
B) Temperature increases, laminar cellular structures (σ and γ_{new}) are formed in phase boundaries.

C) Temperature increases, laminar cellular structures continue to grow.

D) Temperature increases, α phase is completely occupied by secondary phases. (15) (16)

APPENDIX

PRECIPITATION MECHANISM OF AUSTENITIC STAINLESS STEEL



Figures a-d show the precipitation mechanism of σ phase in austenitic stainless steel at different temperatures.

A) Without heating δ ferrite is indicated by a lacy structure that precipitates at the δ/γ boundaries.

B) Temperature increases, σ and γ_{new} (secondary austenite) precipitate in δ ferrite particles.

C) Temperature increases, σ and γ_{new} continue precipitating and σ starts precipitating at the triple points.

D) Temperature increases, precipitation of the lamellar σ and γ_{new} is more obvious. (15) (16)

APPENDIX

APPENDIX G. EQUIPMENT

All equipment was provided by the University of Stavanger.

For machining:



Somatec SCK400+ cold saw



Stamac STF5000V mill

For heat treatment:



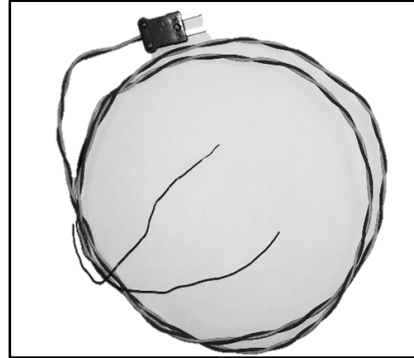
Nabertherm p310 high temperature furnace

APPENDIX

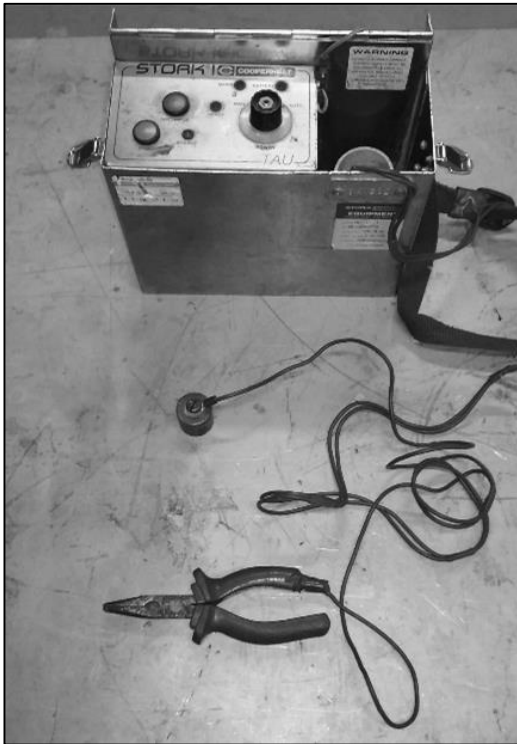
For measuring:



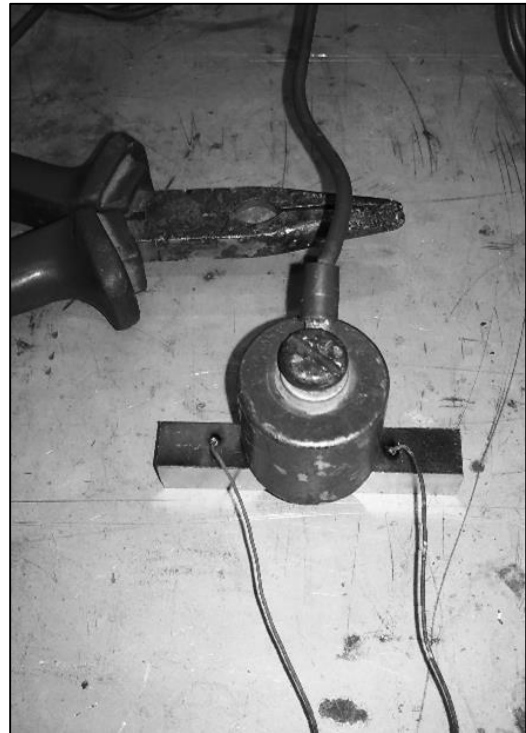
EI-USB-2 thermocouple data logger. Used for logging temperature variations



Heat resistant cable and K-element for logging.



Cooperheat Stork welder. Used to weld in place cable to samples



Sample with welded cable connected to data logger

APPENDIX

For analyzing:



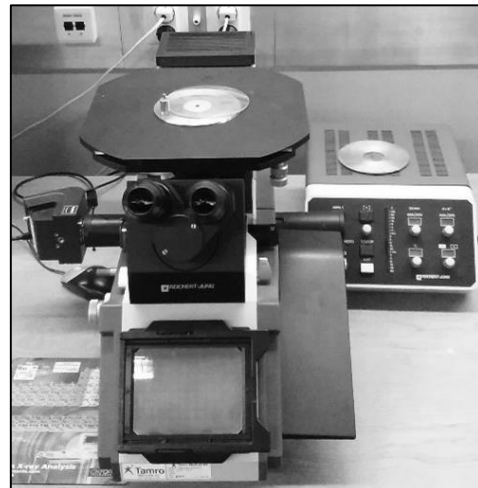
*Zwick-Roell RKP450 Charpy V-notch Impact test machine
450J capacity*



*Struers Planopol pedemax-2 automatic grinder and
polishing machine. Used to prepare samples for
metallographic examination*



*Struers lectropol-5 apparatus for electrolytical etching of
metallographic specimens*



Reichert Jung light optical microscope

APPENDIX

APPENDIX H. ORGANIZATION OF SAMPLES FOR FURTHER STUDIES

All the remaining material, composed by:

- 1,5 pipe sections of UNS S31254
- 1 pipe section of UNS S32760

Are delivered to supervisor Torfinn Havn.

All the collected samples that have been analyzed for this research are organized after “heat treatment” number and after the unified numbering system of the alloy.